Statistical Modelling of Population Evolution

T. D. Preece, BSc.

Thesis submitted to The University of Nottingham

for the degree of Doctor of Philosophy

April 2009

Abstract

In this thesis analytical and simulation techniques are applied to problems in biological evolution. The thesis is divided into four parts.

Firstly, chapter two investigates anomalies that occur in the Penna bit-string model of ageing, an influential model of mutation accumulation and selection. These anomalies result in unusual demographic distributions and can lead to the so-called Eve effect. The anomalies are characterised along with their associated demographic distributions. It is argued that the anomalies are similar in nature to the well known first-passage problem.

Secondly, chapter three uses evolutionary game theory to investigate the evolution of harmful mating tactics in hermaphrodites. These tactics benefit the function of the sperm donor at the expense of sperm recipient. The model predicts evolutionary stable values of resource allocation between sexual functions, and the level of harm. The analysis provides support for empirical observations and makes predictions about the effects of harmful mating tactics on population evolution.

Thirdly, chapter four considers the sustainability of the two main types of

sexual reproduction; hermaphroditism and dioecy (male and female individuals). By use of stochastic spatial simulations it is demonstrated that hermaphroditism can have an even greater advantage over dioecy than predicted by mean-field analysis. This result provides support for the observation that hermaphroditism is associated with sedentary species.

Finally, chapter five considers the evolution of gynodioecy, a breeding system of plants in which populations consist of hermaphrodite and female individuals. It is both a common and widespread polymorphism, and has been identified in many species of ecological and economic interest. Mean-field calculations and stochastic spatial simulations are used to identify the conditions necessary for gynodioecy to evolve.

Publications

Chapter 2

- T. Preece and Y. Mao. Anomalies and the Eve effect in the asexual Penna model. *Physical Review E*, 74(5):051915, November 2006.

Chapter 3

- T. Preece, Y. Mao, J. P. Garrahan and A. Davison. Harmful mating tactics in hermaphrodites. *American Naturalist*, 173(5), May 2009. (Electronically published March 20, 2009)

Acknowledgements

Firstly, I would like to thank the EPSRC for financial support, in the form of a studentship, during the three years I have spent as a postgraduate at the University of Nottingham.

I would like to thank my academic supervisor Dr Yong Mao for his support and guidance thoughout my PhD, and for passing on pearls of wisdom on matters academic and otherwise, it was much appreciated.

Due to the interdisciplinary nature of this thesis, the consultation of Dr Angus Davison from the Institute of Genetics was invaluable. In particular I would like to thank Dr Davison for his collaboration on the work presented chapter 3 of this thesis.

I would like to thank Professor Juan P Garrahan for his collaboration on the work presented in chapter 3 of this thesis and for useful discussion on matters statistical mechanical.

For coming to my aid during times of trouble with the IT network I would like to thank Andrew Wilson and Dr Philip Hawker.

I would like to thank Dr Ian Hands for advice on poster presentations and

tips on software applications to make my life easier, they did.

For useful discussion on mathematics, physics and computing I would like to thank my colleague Douglas Ashton.

For taking my mind off research, I would like to thank the Physics Department's cricket and football teams, in particular Ricky and Lester for starting up the teams.

For allowing me the use of his apartment during the final stages of my thesis preparation I would like to thank Ross Milton. I would also like to thank Ross for organising some fantastic excursions over the past three years.

I would like to thank my unofficial personal trainer Andrew J Pollard for keeping me in fine physical form over the past three years, this has undoubtedly aided my performance at the computer.

I have made many friends during my time in Nottingham who have made my time here very enjoyable. I would like to thank; Nicholas Bridgman for his operatic performances, Richard Fawcett for philosophical conversation, Ben Medford for not so philosophical conversation, Ian Dunlop and Paul Woodward for rugby chat, and all the members of "Anna's tea room cru'!" who play harder than any other physics social group I know.

Finally, I would like to thank my family; David, Margaret, John and Jo, for their love and support. I would also like to thank my family and my grandmother for proof reading passages of my thesis.

Contents

CHAPTER 1

Modelling evolution

1.1 Introduction

Evolutionary studies aim to explain and predict physical, behavioural and genetic changes in biological populations with time. Darwin [1] first proposed that the forces driving these changes were inheritance of traits, from parents to offspring, and natural selection on these traits. Though, Darwin had no knowledge of the genetic mechanism for inheritance. A genetic mechanism for inheritance was first discovered by Mendel through breeding experiments with pea plants [2]. Mendel's laws of inheritance describe the inheritance of a trait that is controlled by a pair of alleles at a single genetic locus, this is known as a Mendelian trait. Mendel's laws state that an individual receives one allele from each parent and that alleles of different genes assort independently. It is now known that independent assortment of genes is only true for traits that are not linked. Genetic linkage occurs when loci are on the same chromosome.

Thus, linked traits may not display the phenotypic distributions predicted by Mendel's laws.

The theories of Darwin and Mendel were unified in what is now referred to as the Modern Synthesis [3]. A key constituent to the Modern Synthesis was the development of population genetics. Population genetics is the study of the evolution of gene frequencies in a population by explicitly mapping genotype to phenotype. Traits considered in population genetics tend to be qualitative in nature, and display discrete variation between phenotypes in a population. In contrast, the field the quantitative genetics considers quantitative traits that usually display continuous variation across a population, for example, height in the human population. A key assumption in quantitative genetics is that these traits are influenced by the interaction of many genes. Although inheritance is based on Mendelian principles, these traits are not Mendelian traits so distributions of phenotypes can not be predicted by Mendel's laws. Thus, genes influencing a particular quantitative trait can not be readily identified. For this reason quantitative genetics is statistical in nature and populations are described in terms of phenotypic means and variances.

In order for selection to act in an evolutionary model, it is necessary to have some measure for the success of an individual who bears a particular trait. This measure is the fitness of an individual and is usually defined as the number of viable offspring produced by that individual. This definition of fitness is used throughout this thesis. The fitness of an individual can be dependent on population size (density dependent selection) and/or dependent on the frequency

of other phenotypes in the environment (frequency dependent selection). For the case where fitness is both density and frequency independent, traits which confer the highest per capita growth rate are selected. If fitness is density dependent and frequency independent, dynamics favours genes that confer the largest carrying capacity, or in other words the gene that maximises population size. When fitness is frequency independent, selection of the fittest trait is an optimisation problem; maximising per capita growth rate or maximising carrying capacity. When fitness is frequency dependent, an individual's fitness depends on other individuals' (opponents) strategies. Thus, the frequency dependent selection case requires a more involved game theoretical analysis.

The frameworks of population genetics and quantitative genetics were the original approaches for modelling evolution in biological populations. Both were derived for the case where fitness is frequency independent, thus they can be described in isolation to evolutionary game theory. In the following sections, population genetics, quantitative genetics and evolutionary game theory are described in more detail.

1.2 Population genetics

In the field of population genetics, populations are described in terms of genotype frequencies and gene frequencies. Genotype frequencies describe the frequency of individuals with a particular genotype. Gene frequencies describe the frequency of alleles at a particular locus in the population.

To incorporate selection it is necessary to map genotypes to a corresponding fitness, this mapping is commonly referred to as the fitness landscape. Consider the case of a single genetic locus in a diploid species for which there are two alleles, B_1 and B_2, with frequencies p_1 and $p_2 = (1 - p_1)$ respectively. The genotype frequencies in the population are p_1^2, $2p_1p_2$ and p_2^2 for the genotypes B_1B_1, B_1B_2 and B_2B_2 respectively. Each genotype is mapped to a fitness, where w_{11}, w_{12} and w_{22} are the fitnesses of the B_1B_1, B_1B_2 and B_2B_2 genotypes respectively. The mean fitness of an individual carrying allele B_1 is thus, $W_1 = p_1w_{11} + p_2w_{12}$, and the mean fitness of the population is given by,

$$\overline{W} = p_1^2w_{11} + 2p_1p_2w_{12} + p_2^2w_{22}. \tag{1.2.1}$$

The simplest, and perhaps the most common, method for evolving the population is to assume that the population is updated in parallel and replaced with a daughter population after one generation. For a population evolving according to this parallel update process, the frequency of allele B_1 in the next generation will be,

$$p_1' = p_1\frac{W_1}{\overline{W}}, \tag{1.2.2}$$

and the frequency of allele B_2 will be,

$$p_2' = p_2\frac{W_2}{\overline{W}}. \tag{1.2.3}$$

If $w_{11} \geq w_{12} > w_{22}$, allele B_2 is eliminated from the population as the population evolves with time. If $w_{12} > w_{11}$ and $w_{12} > w_{22}$, the population maintains both alleles B_1 and B_2. The equilibrium gene frequencies are calculated by solving equilibrium condition, $W_1 = W_2$, with known genotype fitnesses. This

example for evolution at one locus ignores mutation. Mutation can be included in the model described above by adding a rate at which one allele mutates to the other allele during the production of gametes. Addition of a mutation rate generally shifts the equilibrium gene frequencies from those that would be seen in the example above, because mutation and selection need to balance at equilibrium.

The evolution of many beneficial mutations over long periods of time can be modelled by using an alternative approach to population genetics, the adaptive walk [4, 5]. Adaptive walk models assume that the population is homogeneous, in genetic terms, most of the time and that beneficial mutations spread rapidly through the population in comparison to the rate at which they occur. In contrast to population genetic models (which describe evolution of gene frequency), the main aim of the adaptive walk model is to incorporate more complex gene interactions , such as epistasis and pleiotropy, into the evolutionary process to describe statistical properties of the system. Epistasis is the interaction of multiple genetic loci, in which case a trait is affected by several genetic loci. In contrast, pleiotropy describes the case where a single gene influences multiple phenotypic traits. Both epistasis and pleiotropy are thought to be involved in the expression of many traits [6, 7].

In many adaptive walk models an organisms genome is represented by a binary bit-string, this allows for efficient computer simulation and the use of analytical techniques originally derived for use in statistical physics [5]. For example, consider the adaptive walk model introduced by Kauffman [4], where

an organism's genotype is represented by a binary bit-string, γ, consisting of N elements. The fitness contribution of each element, γ_i, is dependent on K other elements, $\gamma_{i_1}, \gamma_{i_2}, \ldots, \gamma_{i_K}$. Thus, the fitness of a configuration γ is given by,

$$W(\gamma) = \frac{1}{N} \sum_i J(\gamma_{i_1}, \gamma_{i_2}, \ldots, \gamma_{i_K}), \tag{1.2.4}$$

where J contains a sum over 2^K spin products. To simulate the adaptive walk, elements are switched ($0 \rightarrow 1$, or $1 \rightarrow 0$) at random; if the resulting genotype is of higher fitness the new configuration is adopted, else it is rejected and another element is switched.

Bit-string representations of genomes have also proved useful when populations cannot be assumed homogeneous. For these problems each individual can be represented by a bit-string and the population evolved according to the mode of reproduction and selection under investigation. Populations represented by binary bit-strings can be modelled very efficiently by computer simulation which allows more complex themes of genetics and evolution to be easily incorporated into models, for example; recurrent mutation [8, 9], epistasis [9], pleiotropy [9], ageing [8] and speciation [10]. This approach is distinct from the population genetic models described above in that the population is no longer described simply by gene-frequencies but by a gene sequence. A bit-sting model which incorporates ageing and recurrent mutation is the subject of chapter 2 in this thesis.

1.3 Quantitative genetics

The field of quantitative genetics is concerned with quantitative traits that are assumed to be influenced by genes at many loci (polygenic), with each gene contributing a small effect to the trait [11]. These quantitative traits usually vary continuously across the population. This contrasts with the discrete nature of traits often associated with population genetic models. Using the assumption that large numbers of genes are responsible for a quantitative trait, quantitative genetics considers these genes in aggregate. This has been likened to the study of systems at the macroscopic level in the physical sciences [12].

The theory of quantitative genetics extends the principles of Mendelian inheritance to accommodate polygenic traits and deduces phenotypic properties on a population level. This is a statistical approach whereby phenotypic variation is decomposed into components of additive genetic variation, non-additive genetic variation and environmental variation. Theory and experiment have a close relationship in quantitative genetics. Empirical data is necessary to determine the properties of the genes associated with quantitative variation, this in turn is used to determine properties such as the heritability of a trait. Experimental breeding then allows the validity of the theory to be tested. This method has proved successful in application to livestock and crop improvement [13].

Quantitative genetics was built upon statistical abstractions of genetic effects, though currently the field is advancing. By utilising recent technological developments, quantitative geneticists aim to reveal explicit links between

genes and complex phenotypes. This synthesis is having a large impact on the areas of evolutionary biology, plant and animal breeding, and the analysis of human disease [14].

1.4 Game Theory

An essential property of any game is that each player's success depends not only on his own strategy but the strategy of others. This differentiates a game problem from an optimisation problem. The theory of games had its beginnings with the two-player matrix game [15]. Matrix games have a finite number of strategy choices, the payoff to each player is determined by an element of a matrix. One player's strategy corresponds to the selection of a row and the other player's strategy corresponds to the selection of a column.

An important concept of game theory is that of the Nash equilibrium [16, 17]. If two opponents adopt the Nash equilibrium strategy neither can increase their payoff by unilaterally deviating from this strategy. For example, consider a case of the well known Prisoner's Dilemma, where two suspects (here called John and Jo) are questioned in separate interrogation rooms. Each suspect is faced with the choice of blaming the other (defect from his accomplice) or remain silent (cooperate with his accomplice). It is reasoned that if both stay silent (cooperate), both will get sentences of 2 years in prison. If one cooperates and the other defects, the cooperator will be sentenced to 5 years and the defector walks free. If both defect, each is sentenced to 3 years. A payoff matrix for John

	Jo cooperates	Jo defects
John cooperates	-2	-5
John defects	0	-3

Table 1.1: Payoff matrix for a Prisonser's Dilemma game. Numbers correspond to years spent in prison.

is given in table 1.1. The payoff matrix for Jo is obtained by swapping the labels John and Jo in table 1.1, thus the game is said to be symmetric.

John and Jo are in Nash equilibrium if both choose to defect because neither can increase his payoff by unilaterally deviating from this strategy. Thus, 'defecting' is the Nash equilibrium strategy for this game.

Evolution by natural selection is a game in the sense that it has players (organisms), strategies (phenotypic traits) and payoffs (fitness). Several features distinguish evolutionary game theory from classical games like the Prisoner's Dilemma described above. In classical game theory, the focus is on the players who aim to choose strategies that optimise their payoffs, thus rationality or self-interest provides the optimising agent for strategy selection. In evolutionary games, strategies are inherited and natural selection serves as an optimising agent. The focus of evolutionary games is on strategies that persist with time.

In an evolutionary game, the fitness of an individual directly influences the frequencies of strategies present in the next generation. Consider the Hawk-Dove game [18], where a population consists of two phenotypes, hawk and dove, and all individuals are competing for favourable territory. An individ-

	Dove	Hawk
Dove	$\frac{V}{2}$	0
Hawk	V	$\frac{V-C}{2}$

Table 1.2: Payoff matrix for the Hawk-Dove evolutionary game.

ual can produce V extra offspring if it occupies favourable territories (wins contest) when compared to the number of offspring it produces if it occupies unfavourable territories (loses contest). During a pair-wise contest a dove will display its interest in the territory but retreat if its opponent wishes to escalate to a potentially harmful fight. In contrast a Hawk will always escalate in the contest and will continue until injured or its opponent retreats. A dove-dove contest results in one of the individuals winning the territory by pure chance, a hawk-dove contest results in the hawk winning the territory, and a hawk-hawk contest results in one hawk winning the territory but the other losing and sustaining damage. This damage is deemed to cost the loser in fitness terms an amount C. The payoff matrix for this game is given in table 1.2.

The payoff matrix for the Hawk-Dove game (table 1.2) shows that a population of doves would always be invaded by a small number of hawks because a member of the resident population of doves would receive a payoff of $V/2$ compared to the payoff of V for the invading hawks. The invading hawks would have a greater per capita growth rate and would grow in frequency. In contrast, a population of hawks would be stable against invasion by a small number of doves if $(V - C)/2 > 0$. Thus, if $(V - C)/2 > 0$, the hawk strategy is said to

be an Evolutionary Stable Strategy (ESS). The ESS is a solution concept for evolutionary games defined by Maynard Smith and Price [19] as; a strategy such that, if most members of the population adopt it, there is no mutant strategy that would give higher reproductive fitness. They reasoned that such a strategy would be stable under natural selection.

It has been recognised that the ESS definition is equivalent to the Nash equilibrium of classical game theory. A Nash equilibrium and an ESS are 'no regret' strategies in the sense that if everyone in a population is playing a Nash strategy (in a classical game) or an ESS (in an evolutionary game), then no one individual can benefit from unilaterally changing their strategy. In the absence of an ESS, a mixed state where multiple phenotypes coexist may be stable. This is the case in the the Hawk-Dove game when $(V - C)/2 < 0$. Other games, such as the game of rock-paper-scissors [20], can exhibit stable cyclic behaviour.

The Hawk-Dove game described above is an example of a discrete evolutionary game. Another type of evolutionary game is the continuous evolutionary game, where strategy sets are continuous and payoff is given by some function of the strategies. For example, in chapter 3, a continuous evolutionary game is considered where a hermaphrodites strategy is the fraction of its resources allocated to its male function, $r \in [0, 1]$. The ESS is an end point of evolution by natural selection as small numbers of mutants cannot invade the population once the ESS is established. However, it is also important to determine whether the ESS is attainable through evolution by natural selection. This can be determined by approximating the strategy dynamics of a popula-

	ESS	not ESS
Convergent	CSS	Branching Point
not Convergent	Garden of Eden	Invasible Repellor

Table 1.3: Types of equilibrium.

tion. Strategy dynamics describe how the strategy used by a population evolves over time in a continuous game, this is a result of changes in the underlying phenotypes present in the population. Dynamical equations governing strategy dynamics are introduced in chapter 3. If the strategy dynamics converge on a particular strategy, this strategy is said to exhibit convergent stability.

The two stability concepts of ESS and convergent stability are independent of each other [21]. Thus, four different equilibria can be classified, these are summarised in table 1.3. Strategy dynamics converge on a Continuously Stable Strategy (CSS) [22]. Once a population adopts the CSS, it is resistant to invasion by a small number of mutant strategies. These are the strategies which would be expected to be observed in nature. Strategy dynamics converge on the branching point, though, at the branching point the population can be invaded by mutants. It is thought that this could lead to speciation. At a Garden of Eden point a population is stable against invasion, however if the population strategy is perturbed away from this point strategy dynamics will evolve away from the Garden of Eden point. A population will always evolve away from and invasible repellor, even if the bulk population is initially at the equilibrium point.

Evolutionary game theory relies on the basic assumption that like begets like, thus does not include any explicit genetic mechanism of trait inheritance. This may appear a short coming when compared to the explicit nature of population genetics, however, game theory is a useful technique for calculating the phenotypes (strategies) that would be expected to evolve in a population and for uncovering reason for the evolution of particular phenotypes [18]. Also, it is often the case that the underlying gentics responsible for a trait are unknown. There are some applications of evolutionary game theory which include explicit genetic detail, however these tend to be less common [18, 23].

1.5 Summary

In chapter 2, computer simulation and an analytical approach are used to investigate the origin and consequences of certain anomalies which have been observed in the Penna model of biological ageing. Penna's model is a model of mutation accumulation and selection where each individual's genome is represented by a binary bit-string.

In chapter 3, an evolutionary game theory model is derived to investigate the evolution of harmful mating tactics in hermaphrodites. Analysis of this model yields the conditions under which harmful mating tactics would be expected to evolve and the consequences of harmful mating on other aspects of population evolution.

In chapter 4, stochastic spatial simulations and mean-field analysis are used

to investigate the stability of hermaphrodite and dioecious (separate male and female individuals) populations. This investigation doesn't consider coevolution or invasion but the robustness of the two mating strategies to extinction.

In Chapter 5, stochastic spatial simulations and mean-field analysis are used to investigate the conditions necessary for gynodioecy to evolve. Gynodioecy is a breeding system of plants in which populations consist of hermaphrodite and female individuals. The model derived explicitly describes the underlying genetics for the case of a dominant nuclear allele conferring male sterility.

CHAPTER 2

Anomalies and the Eve Effect in the Asexual Penna Model

2.1 Introduction

In 1995, T. J. P. Penna [8] proposed a binary bit-string computational model for the process of evolutionary ageing. The model is deceptively simple to construct, and yet it captures some key features of evolution, namely, mutation accumulation and selection. Indeed, the basic Penna model provides a useful foundation upon which other effects could be added and studied [24]. As a result, the Penna model has acquired a considerable popularity, and over 200 published citations of the original 1995 article can be found at the time of writing.

The idea that the natural selection, and therefore the survival of the fittest, seemingly contradicts the detrimental behaviour of ageing and the general de-

cline of an organism's capability [25]. The resolution of this conflict lies in the occurrence of mutations. It is now generally accepted that ageing is regulated by specific genes, as originally proposed by Medawar [26], and their effects depend on the reproductive life cycle of the individual organism as well as random mutations that occur [27]. The Penna model [8] provides a means to model this delicate interplay during the evolution of an age-structured population under the influence of age-specific harmful mutations [24].

The original Penna model is designed for computer simulations, and therefore is discrete in nature. Time steps are counted by an integer and an organism's genome represented by a binary bit-string. Each 0 on the bit-string represents a healthy site, and each 1 a harmful one. The location of the harmful sites on the bit-string, indicate the ages at which the organism suffers the harmful effect (a disease). Having suffered T_d diseases an organism dies. The bit-string is of course finite in length (usually 32 or 64 bits as dictated by the available 32-bit and 64-bit computer processors) and each newborn inherits the parental string, with extra mutations introduced into its bit-string.

An early success of the Penna model was accounting for the catastrophic senescence found in Pacific salmon[28]. The model demonstrated that the only condition required for catastrophic senescence to emerge is a semelparous reproductive strategy, which means that the organism reproduces just once during its lifetime. Salmon only mate once in their life-time at a specific age, any individual with too many diseases prior to this age will never reproduce. The combination of the selective pressure up to this reproductive age and the lack

of selection following this age leads to catastrophic senescence shortly after reproduction.

Another interesting application of the Penna model was simulating the advancements in medical care over the last century by steadily increasing the disease threshold T_d. Laszkiewicz *et al* [29] reasoned that changes in mortality over this period are not due to changes in the genetic population because human lifespan is too long compared to the period of time. They found a reasonable match of their simulation results for mortality with recorded results for the American population between the years 1870 and 1980. Penna's model has also been able to reproduce important demographic features, such as exponentially increasing mortality with age [30] (the so-called Gompertz Law [25]), and mortality plateau for the oldest old[31, 32].

In sexually reproductive species the production of males who can't carry offspring constitutes a two-fold cost of sexual reproduction when compared to asexual reproduction. There is heated debate [33] as to how and why sexual reproduction has emerged given this two-fold cost. Due to its bit-string nature, genetic recombination and mutation are very easy to model using the Penna model and Penna's model has been used to identify regimes in which sexual reproduction is favourable [34, 35].

The asexual Penna model has been formulated and solved [31, 36]. The case of $T = 1$ gives straightforward agreement between computer simulation and analytical solution. For $T_d > 1$, the analytical solution was obtained through the ansatz that the positions of non-terminal deleterious bits (the first $(T_d - 1)$

deleterious bits) are not significant in determining the sizes of subpopulations of a given genetic lifespan l. Agreement between this analytical solution and computer simulations is observed, for $T_d > 1$, provided that simulation size is very large and simulation period is relatively short. With moderate parameters however, computer simulation can frequently lead to a host of distinct steady states. These are indicative of certain anomalies, which are analysed in the following sections.

Many simulations using the asexual Penna model with disease threshold greater than one ($T_d > 1$) have noted discontinuities when plotting the frequency of diseased bits versus genetic location for a population [34, 37]. This was also manifested in mortality plots as discontinuous jumps in an otherwise smooth curve. The locations of these discontinuities was found to vary even for simulations run with same model parameters and initial conditions. Sá Martins *et al* [34] attributed these discontinuities to the fixation of mutations at certain loci, but did not suggest a mechanism for fixations to emerge. Most previous simulations of the Penna model have used a disease threshold greater than one, making them susceptible to these anomalies.

Section 2.2 describes simulation of the asexual Penna model in more detail. An analytical solution for the multiple disease Penna model and an explanation of the origins of the anomalies observed for $T_d > 1$ is presented in section 2.3. For the purpose of clarity, the analysis presented here concentrates on the case of $T = 2$. For higher threshold values of T_d, the anomalies remain qualitatively the same.

2.2 The asexual Penna model

During each simulation time step every individual's bit-string is inspected to check for new heritable diseases then the organisms age is incremented. A diseased (1) bit at location i on the organisms bit-string affects the individual at age i. On accumulating T_d diseases an individual dies. Thus, an individual with its T_dth diseased bit located at postion 10 on its bit-string (bits are indexed from zero) will live for 10 time steps in the simulation. During each time step, each individual reproduces with a probability b. There is a probability of error in the replication process attributed to random mutation occurring with probability P_m per location on the bit-string. For ease of notation P_m is written as $1 - e^{-\beta}$, where β is referred to as the mutation rate. This is a common convention used in the literature.

Mutations are considered as always harmful (turns a 0 into a 1), since harmful mutations vastly outnumber the helpful ones in nature [27]. This assumption may be relaxed to allow a small rate of positive mutation which does not qualitatively alter the overall picture [38]. Therefore, here only single harmful mutations at births are considered. If a location already set to 1 is selected for a mutation it remains 1.

To maintain a finite population size a Verhulst-factor [39] birth rate is used, $b(t)$, given by,

$$b(t) = b_0(1 - N(t)/N_{max}), \tag{2.2.1}$$

where b_0 is a constant, $N(t)$ is the population size at time t and N_{max} is the

carrying capacity of the environment.

Deleterious mutation during reproduction results in an offspring with a shorter genetic lifespan than its parent. As subpopulations of a given genetic lifespan, l, receive input due to mutation from populations of longer genetic lifespan, there must exist a subpopulation of longest genetic lifespan, l_{max}, capable of maintaining itself. Thus, the expected number of unmutated offspring produced by an individual of genetic lifespan l_{max} over its lifetime must be one,

$$l_{max} b e^{-\beta(l_{max}-T_d+1)} = 1, \tag{2.2.2}$$

where b is the steady state birth rate. This steady state birth rate is reached quickly in the simulation, and the birth rate varies relatively little after reaching equilibrium. Also, if the population is to remain bound, for any subpopulation of $l < l_{max}$ the expected number of unmutated births by an individual during its lifetime must be less than one,

$$(l_{max} - 1) b e^{-\beta[(l_{max}-1)-T_d+1]} < 1. \tag{2.2.3}$$

Rearrangement of equation 2.2.2 gives the steady state birthrate for a given l_{max},

$$b = \frac{e^{\beta(l_{max}-T_d+1)}}{l_{max}}. \tag{2.2.4}$$

Substituting equation 2.2.4 into equation 2.2.3 gives the constraint on l_{max},

$$l_{max} < \frac{1}{(1 - e^{-\beta})}. \tag{2.2.5}$$

Equation (2.2.5) is particularly useful when choosing simulation parameters as l_{max} should be less than 32 or 64, depending on the processor being used.

2.3 Analytical solution and simulation results

For the $T_d = 2$ case, the first 2 deleterious bits, l_1 and l (with $l > l_1$), are of interest. The second bit at l marks the death of the individual and thus l is referred to as the genetic lifespan. A population can be characterised in terms of the population distribution function $n(l_1, l)$, defined as the number of individuals with their first 2 deleterious bits located at l_1 and l.

Figure 2.1 presents a typical scenario of $n(l_1, l)$ from a computer simulation of a population after reaching steady state. Simulation parameters are; mutation rate $\beta = 1/30$, birth rate is given by the Verhulst birth rate with $b_0 = 1$, the maximum population $N_{max} = 10^7$, and $l_{max} = 16$ represents the maximum genetic lifespan of the population.

A notable feature in figure 2.1 is the formation of a ridge at $l = 11$. The population as a function of genetic lifespan l can be obtained by summing $n(l_1, l)$ over l_1,

$$n(l) = \sum_{l_1} n(l_1, l), \tag{2.3.1}$$

then the aforesaid ridge gives rise to a spike in the corresponding $n(l)$ plot, as presented in figure 2.2 (all simulation parameters for figure 2.2 are the same as for figure 2.1). The spike is located at the postion of the ridge, $l_s = 11$. This is in stark contrast to predictions using the ansatz, that positions of non-terminal deleterious bits are not significant in determining the sizes of subpopulations, which gives rise to a smooth curve for $n(l)$, shown to be valid for very large

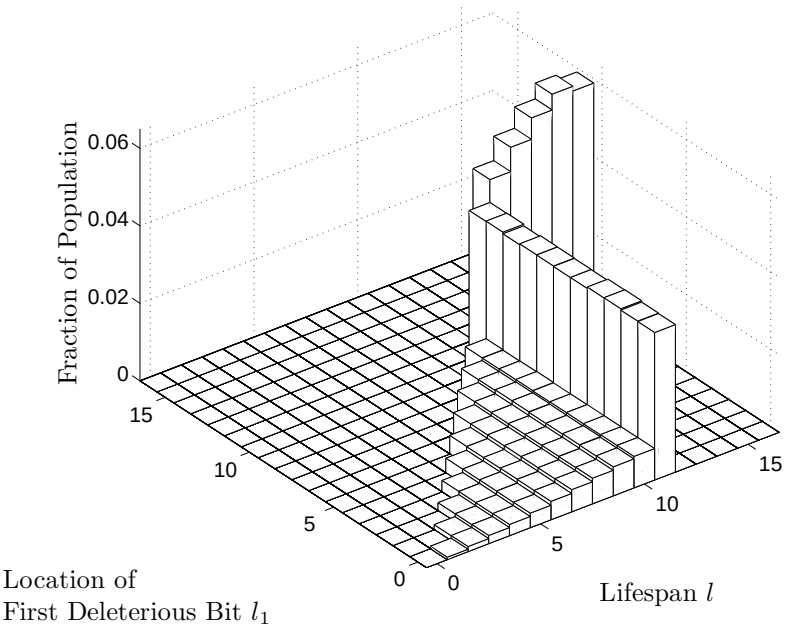

Figure 2.1: Simulated population $n(l_1, l)$ versus the location of the first deleterious bit l_1 and the genetic string length l.

populations over short simulation times [31].

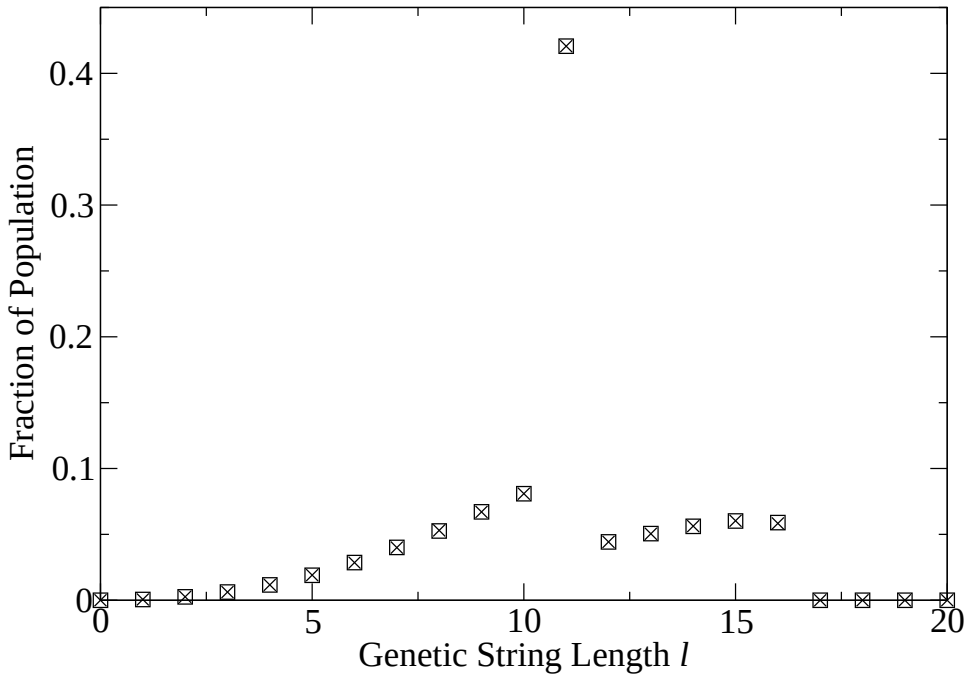

Figure 2.2: Fraction of population with genetic string length l, $n(l)/\sum_{l'} n(l')$; from simulation (□) and analytical solution (×), showing excellent agreement.

Further simulations show that the spike location l_s appears to be developed randomly for repeated simulations with the same set of initial conditions. Once the spike forms, its location l_s becomes fixed. Furthermore, the population $n(l_1, l)$ dies out completely for the case $l_1 > l_s$, and the case $l_1 < l_s$ and $l > l_s$. Guided by these observations, we formulate our analytical approach step by step for $l > l_s$, $l = l_s$, $l < l_s$, as follows.

For $l > l_s$; since a population with $l_1 > l_s$ dies out, those organisms with

$l_1 = l_s$ obey the following evolution equation,

$$\frac{dn(l_s,l)}{dt} = be^{-\beta(l-1)}n(l_s,l) - \frac{n(l_s,l)}{l} + bP_m e^{-\beta(l-1)} \sum_{l'=l+1}^{l_{max}} n(l_s,l') \qquad (2.3.2)$$

where b and β are rates for birth and mutation respectively; P_m is the probability of mutation at a given site $P_m = 1 - e^{-\beta}$; and l_{max} is the maximum l of the population. The first term on the right hand side results from mutation free births, the second term from death and the third term from mutated births. This formulation is similar to the $T = 1$ case of the standard Penna model [31]. For steady state, the time derivative d/dt goes to zero, and our evolution equation can be solved exactly by the recursion relation,

$$\frac{n(l_s,l+1)}{n(l_s,l)} = \frac{l+1}{l} \frac{e^{\beta(l-1)} - bl}{e^{\beta l} - b(l+1)e^{-\beta}}. \qquad (2.3.3)$$

Thus, given the population $n(l_s, l_{max})$, we can determine all $n(l_s, l)$ for $l_s < l < l_{max}$. The model is linear and scalable, so the distribution function $n(l_1, l)$ can be normalised later to give results in terms of the fraction of the population with a genotype (l_1, l).

For $l = l_s$; the mutated births into $l = l_s$ can only come from those $n(l_s, l)$ with $l_s < l \leq l_{max}$, since only single harmful mutations are considered. Thus, the evolution equation for population $n(l_1, l_s)$ reads:

$$\frac{dn(l_1,l_s)}{dt} = be^{-\beta(l_s-1)}n(l_1,l_s) - \frac{n(l_1,l_s)}{l_s} + bP_m e^{-\beta(l_s-1)} \sum_{l'=l_s+1}^{l_{max}} n(l_s,l'). \quad (2.3.4)$$

Again setting the time derivative to zero for steady state, yields the solution

$$n(l_1,l_s) = \frac{bP_m l_s}{e^{\beta(l_s-1)} - bl_s} \sum_{l'=l_s+1}^{l_{max}} n(l_s,l'), \qquad (2.3.5)$$

where the sum is given by the solution $n(l_s, l)$ from the previous $l > l_s$ case. Note that right hand side does not contain l_1, thus our analysis predicts that $n(l_1, l_s)$ is independent of l_1. In other words, the ridge in figure 2.1 should be level, a prediction confirmed by simulations.

For $l < l_s$; population $n(l_1, l)$ can be enhanced by mutated births from either $n(l_1, l')$ or $n(l, l')$ with $l' > l$, so

$$\begin{aligned} \frac{dn(l_1,l)}{dt} &= be^{-\beta(l-1)}n(l_1,l) - \frac{n(l_1,l)}{l} \\ &\quad + bme^{-\beta(l-1)} \sum_{l'=l+1}^{l_s} \left[n(l_1,l') + n(l,l')\right]. \end{aligned} \tag{2.3.6}$$

Noting that this equation, in fact, remains true for all $l_1 < l$, we deduce that the solution $n(l_1, l)$ will be independent of l_1. This deduction is confirmed by the simulation results shown in figure 2.1, and therefore, equation (2.3.6) can be solved analytically yielding the following recursion relation,

$$\frac{n(l_1, l+1)}{n(l_1, l)} = \frac{l+1}{l} \frac{e^{\beta(l-1)} - bl}{e^{\beta l} - b(l+1)(2e^{-\beta} - 1)}. \tag{2.3.7}$$

Combining the above three stages of analysis, the entire distribution of population can be calculated. Finally, normalisation can be applied to give results in terms of the fraction of the population with a genotype (l_1, l), thus independent of simulated population size.

Our analytical results have been plotted in figure 2.2, together with the data from simulation. The excellent agreement validates the theoretical formulation and the mechanisms it reveals of the population dynamics in the Penna model.

2.4 Discussion

The standard Penna simulations only consider a possible single negative mutation at birth as the dominant mutation mechanism. This in turn limits the interaction between different genotypes. For a steady state to exist there must be a longest lived subpopulation which is self-sustaining, *i.e.* not reliant on mutated births. No other shorter-lived subpopulation can be self-sustaining if the population is to remain bounded, as shorter-lived organisms can always be created by mutated copies of longer-lived ones. For the longest-lived subpopulation to be self-sustaining, each organism must produce one perfect copy of itself during its lifetime. All other populations, with $l < l_{max}$, gain from mutated births of the longest lived, so unmutated birth per individual must, on average, be less than unity.

In simulations, birth rate is modified by the so called Verhulst factor, and when the steady state is reached the birth rate would be such that the organism with $l = l_{max}$ produces exactly one mutation-free copy of itself during its lifetime. For $T = 1$, there is no ambiguity to the longest living genotype $n(l_{max})$, but for $T = 2$ however, it is possible for two individuals to have different locations for their first deleterious bit whilst having the same $l = l_{max}$ and the same lifespan. Moreover, if $l_1 \neq l_1'$, a subpopulation $n(l_1, l_{max})$ can never give rise to $n(l_1', l_{max})$ through a single negative mutation. Therefore, the genotype (l_1, l_{max}) would evolve somewhat independently from (l_1', l_{max}). In fact, the evolution equation (2.3.2) is identical to the earlier ansatz solution for $T = 2$

[31].

In the case of $T = 1$, extinction of the l_{max} subpopulation is alleviated by the Verhulst factor which increases the birth rate when the total population drops. But for $T = 2$, all subpopulation $n(l_1, l_{max})$ for different l_1's fluctuate due to the stochastic nature of the simulation, much like a collection of diffusing particles under an overall constraint due to the Verhulst factor. But the Verhulst factor only acts on the total population, and each subpopulation can easily become extinct as another subpopulation can grow to make up the total population. When a subpopulation $n(l_1, l_{max})$ ventures close to extinction, it receives little help towards a recovery, and the closer it is to extinction the more vulnerable it becomes. Therefore, given enough time, the system would eventually settle into one of subpopulations which gives rise to the spiked states observed in simulations. This is akin to the first-passage problem of multiple diffusive particles [40, 41].

Once the population has evolved to contain a unique longest lived subpopulation (l_s, l_{max}), it is still possible for this subpopulation to become extinct due to the stochastic nature of the simulation. However, the timescale for this to occur is far longer than the time taken for the population to reach a state with a unique longest lived subpopulation. It should also be recognised that over long enough timescales the entire population could become extinct. However, neither of these two events were observed for the parameters used in the investigations described here, the spiked state was stable over very long simulation times.

By labelling each individual in the initial population with a number and ensuring this identifier is passed on to offspring, at any subsequent time, an individual can be identified as being a descendant of one of the original population. Thus individuals can be thought of as belonging to a particular family. Figure 2.3 plots the number of distinct genetic families versus time, showing a steady decline, and leading to the "Eve effect" [37, 42] (all individuals are descendants of one member of the initial population). This is in broad agreement with previous results [37] reporting potential scaling regimes of -1 and -2. However, it should be noted that the scaling does not persist over a significant range as is the case in reference [37], and the early time behaviour is particularly sensitive to initial conditions.

Figure 2.4 gives a histogram of time taken to reach a spiked population configuration from 1600 repeated simulations under the same initial conditions. The simulation parameters are: $\beta = 1/30$, $b_0 = 1$, $N_{max} = 4.5 \times 10^4$ and $l_{max} = 16$. The resulting histogram is very similar to the survival time distribution, the so-called Smirnov density, of the first-passage problem [40, 41]. Larger populations give rise to a longer survival time, in accordance with the first-passage problem solution. Due to the presence of the Verhulst factor, which in effect introduces interaction between the diffusing particles, a direct comparison is not legitimate and the Smirnov density function did not give a good fit of the simulation results in figure 2.4 (fit not shown). In practise, the Verhulst factor varies relatively little after the early stage simulation steps during which a steady total population is achieved. This explains why figure 2.4 closely re-

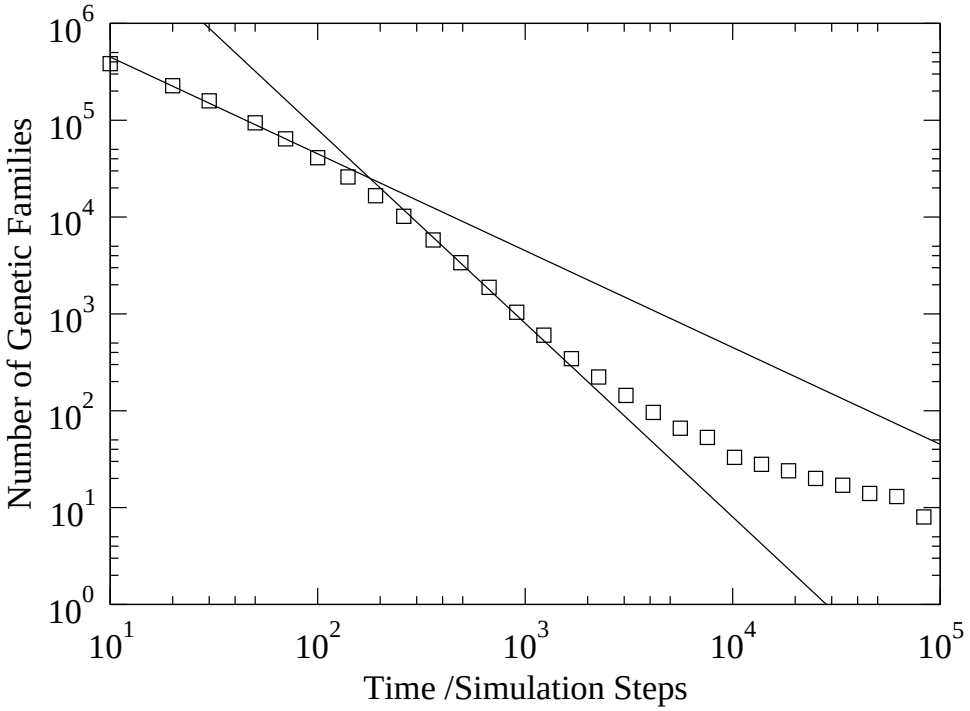

Figure 2.3: The decline of the number of distinct genetic families versus time, leading to the "Eve effect". The two straight lines have slopes -1 and -2.

sembles the first-passage survival time distribution.

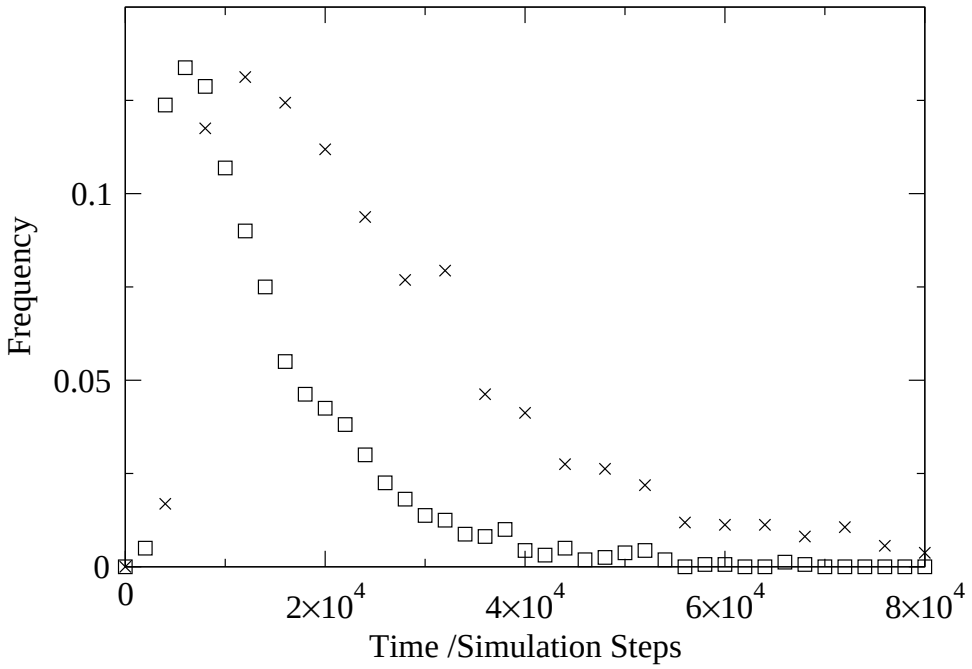

Figure 2.4: Histogram of normalised frequency versus time to complete spike formation. Simulation parameters are $\beta = 1/30$, $b_0 = 1$, $l_{max} = 16$ with $N_{max} = 2.25 \times 10^4$ (□) and $N_{max} = 4.5 \times 10^4$ (×).

Figure 2.5 shows the occurrence frequency of the different locations of the spikes in 1600 repeated simulations. The simulation parameters are the same as those of figure 2.4 with $N_{max} = 4.5 \times 10^4$. Figure 2.5 shows that the probability distribution for the location of l_s is uniform, thus we can conclude that location l_s is indeed random, as our analysis would suggest. The formation of the spiked population configurations clearly reduces the diversity in lineage, as a large number of subpopulations are in effect wiped out during the spike formation.

Different power laws were observed for early and late stage simulations of the "Eve effect" [37, 42]. This difference, according to our analysis, could be linked to the variation within (and the lack of) the Verhulst factor at the early and late stage simulations.

Finally, for cases where $T > 2$, we find qualitatively similar anomalies in simulations. The analytical formulation follows a similar line as presented here, with the population $n(l_1, l)$ generalising to $n(l_1, l_2, l)$.

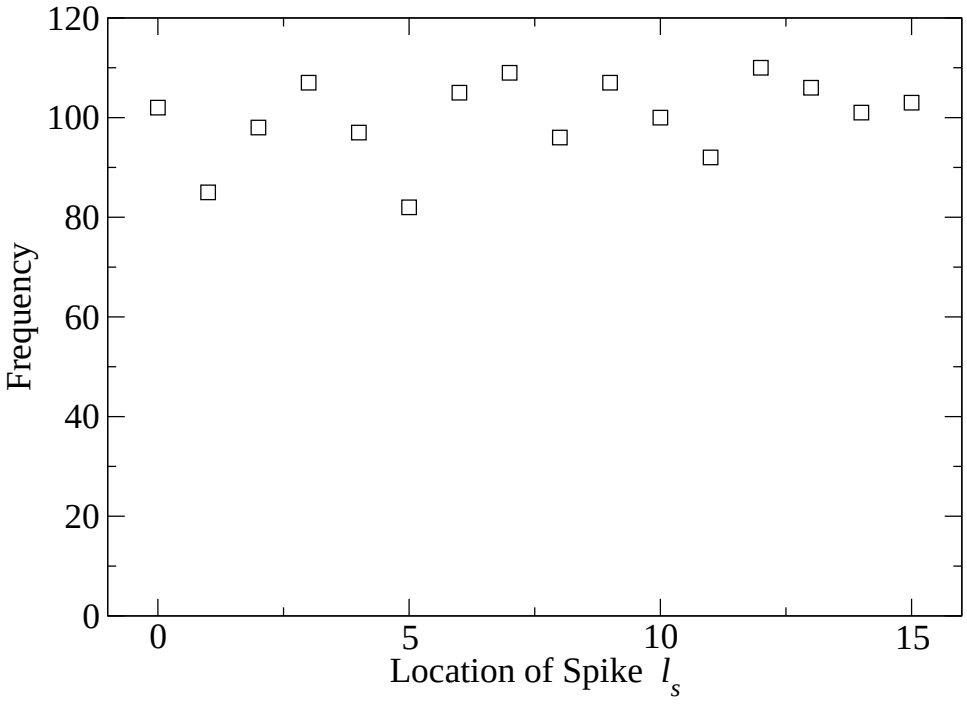

Figure 2.5: Distribution of the spike location l_s.

2.5 Conclusions and future investigations

It has been shown by means of exact analytic solution and computer simulation that, in the asexual Penna model, a series of anomalies exist which may have affected all similar Penna simulations in the past. These anomalies and their associated demographic distributions were characterised. Future simulations of the asexual Penna model need to pay special attention to these anomalies if reliable results are to be obtained. The analysis presented here also suggests that the so-called Eve effect arises in the Penna model via a mechanism similar to the first-passage problem.

In the future, the Penna model could be a useful tool for investigating effects

of age and epistasis in disease. Over the past two decades genetic screening has been successful in identifying genes associated with Mendelian diseases (diseases associated with one genetic locus) [43]. However many diseases, such as Alzheimer's disease [44] and type 2 diabetes [45], appear to be influenced by multiple genetic loci. Currently, there is much research interest in identifying loci associated with increased risk to these diseases [43, 46, 47]. In the related area of evolution of complex genetic traits, a binary bit-string model of mutation and selection (though not age structured) has been utilised to investigate the way in which a population moves through sequence space for a variety of fitness landscapes [9]. The landscapes used are similar to the Kauffman's NK model [4], and adaptive walks were used to characterise the landscape prior to population dynamical simulations. Simulations of this type increase understanding of the evolution of complex traits and may indicate likely associations in empirical data. The Penna model could be used in a similar manner to investigate the evolution of diseases which result from the interaction of multiple genetic loci.

CHAPTER 3

Harmful Tactics in Mating

3.1 Stability in Evolutionary Games

The two stability concepts for evolutionary games, the ESS and convergent stability, were introduced in 1.4. Here the ESS and convergent stability are described in the context of evolutionary games with continuous strategy sets (continuous evolutionary games). In this section methods are presented for characterising equilibria in terms of the ESS and convergent stability. These methods are later applied to the evolution of harmful mating tactics in hermaphrodites.

3.1.1 The Evolutionary Stable Strategy

Maynard Smith defined an Evolutionary Stable Strategy (ESS) as a strategy such that, if most of the members of a population adopt it, there is no mutant strategy that would give higher reproductive fitness [18, 19, 48]. Here, ESS conditions are described for a continuous evolutionary game. To test whether a strategy r

is an ESS, it is necessary to construct a function , $W(\hat{r}, r)$, which describes the fitness of a rare mutant using strategy $\hat{r}$ living in a population which uses strategy r. As the mutant is rare it is approximated that it only interacts with members of the resident population (using strategy r). Following Maynard Smith's definition of the ESS, a sufficient condition for a strategy to be an ESS is,

$$W(\hat{r}, r^*) < W(r^*, r^*) \qquad \forall\, \hat{r} \neq r^*, \tag{3.1.1}$$

where r^* is the ESS. It is common notation to mark an ESS with an asterisk and is used throughout this thesis.

Generally a strategy set will be bound. Strategies lying on the boundaries of the strategy set will be referred to as boundary strategies and strategies lying between the boundary strategies will be referred to as interior strategies. From equation (3.1.1), it can be seen that an interior strategy is an ESS if,

$$\left.\frac{\partial W(\hat{r}, r^*)}{\partial \hat{r}}\right|_{\hat{r}=r^*} = 0, \tag{3.1.2}$$

and

$$\left.\frac{\partial^2 W(\hat{r}, r^*)}{\partial \hat{r}^2}\right|_{\hat{r}=r^*} < 0. \tag{3.1.3}$$

The lower bound of the strategy set is an ESS if,

$$\left.\frac{\partial W(\hat{r}, r^*)}{\partial \hat{r}}\right|_{\hat{r}=r^*} < 0. \tag{3.1.4}$$

Inequality in equation (3.1.4) is reversed for the case of the upper bound of the strategy set.

ESSs are end points in an evolutionary process. Once established, a population using the ESS is stable against invasion by a small number of mutant

strategies. Next, convergent stability is considered, this can test whether an ESS is attainable through evolution, if the population originally uses an alternative strategy.

3.1.2 The G-function approach and strategy dynamics

A similar framework to that described above (in section 3.1.1) was derived by Vincent *et al.* [21], who introduced the fitness generating function (G-function). This approach is particularly useful when considering a symmetric evolutionary game with many phenotypes. Consider an environment consisting of N_p different phenotypes. The per capita growth rate, $H_i(\mathbf{u}, \mathbf{x})$, for phenotype i is a function of all the other phenotypes in the environment, $\mathbf{u} = (\mathbf{u^{(1)}}, \ldots, \mathbf{u^{(N_p)}})$, and the density of each phenotype, $\mathbf{x} = (\mathbf{x^{(1)}}, \ldots, \mathbf{x^{(N_p)}})$. This per capita growth rate includes the fitness of the individual and death rate. The population dynamics are given by,

$$\frac{dx^{(i)}}{dt} = x^{(i)} H^{(i)}(\mathbf{u}, \mathbf{x}). \tag{3.1.5}$$

A G-function is defined as follows [21]: a function $G(v, \mathbf{u}, \mathbf{n})$ is fitness generating function for the population if and only if,

$$G(v, \mathbf{u}, \mathbf{x})|_{v=u^{(i)}} = H^{(i)}(\mathbf{u}, \mathbf{x}), \qquad \mathbf{i} = \mathbf{1}, \ldots, \mathbf{N_p}, \tag{3.1.6}$$

where $u^{(i)}$ is the strategy of phenotype i and v is referred to as a virtual strategy. The per capita growth rate for a strategy $u^{(i)}$ can be obtained by substituting $v = u^{(i)}$ into the G-function. The population dynamics for the phenotype i are

then given by,

$$\frac{dx^{(i)}}{dt} = x^{(i)}\, G(v, \mathbf{u}, \mathbf{x})\big|_{v=u^{(i)}}\,. \tag{3.1.7}$$

Consider a population consisting of only one phenotype u; the ability of this population to resist invasion by a small number of mutant phenotypes (the condition for ESS) can be tested by constructing the G-function, $G(v, u, x)$. The condition for a strategy, u, to be an ESS, u^*, is [49],

$$G(v, u^*, x) < G(v, u^*, x)\big|_{v=u^*} \qquad \forall\, v \neq u^*. \tag{3.1.8}$$

This is similar to the condition for an ESS in equation (3.1.1). The dependence on x can be dropped from equation (3.1.8) for cases of one resident phenotype where selection is density independent. This is indeed the case for the harmful mating model considered later in this chapter. The virtual strategy v in the G-function approach plays the same role as the rare mutant strategy $\hat{r}$ in the invasion analysis described above.

The G-function approach has been utilised to approximate the evolution of strategies used by a population [21, 50]. These strategy dynamics were derived by considering a species to consist of a local distribution of strategies about some mean. The pay-off for using a particular strategy in the distribution is approximated by playing it against the mean strategy of the local distribution of strategies. Populations of individuals with higher fitness grow quicker, thus the mean strategy evolves in the direction of the fitness gradient as,

$$\frac{du}{dt} = \eta\, \frac{\partial G(v, u)}{\partial v}\bigg|_{v=u}. \tag{3.1.9}$$

where u now represents the mean strategy of the local distribution of strategies

and η is the variance in u. A rigorous derivation of equation 3.1.9 is given in references [21, 51]. These dynamics are in agreement with other derivations using similar arguments [22, 52]. Equilibria for the strategy dynamics can be found by solving equation (3.1.9) with the time derivative set to zero. If the strategy dynamics, given by equation 3.1.9, converge on a point (equilibrium or boundary), this point is said to display convergent stability. Convergent stability can be global or local according the the basin of attraction for a given equilibrium. An example of strategy dynamics converging on an interior ESS is shown in figure 3.1. The fitness function in this example is taken from a model for resource allocation between male and female sexual functions in hermaphrodites [53].

In nature many traits do not evolve in isolation but are affected by the evolution of other traits. A game theoretical approach for coevolution requires the introduction of vector strategies (strategies with multiple components). For example, later in this chapter a model for harmful mating tactics is derived where resource allocation between sexual functions and level of harm are the two strategy components.

Strategy dynamics have been extended for populations with multiple species and vector strategies (strategies with multiple components) [21, 50]. Assuming heritable independence between components of a vector strategy, the strategy dynamics for a two component vector strategy is given by,

$$\frac{du_1}{dt} = \eta_1 \left. \frac{\partial G(v_1, v_2, u_1, u_2)}{\partial v_1} \right|_{v_1=u_1, v_2=u_2} \tag{3.1.10}$$

$$\frac{du_2}{dt} = \eta_2 \left. \frac{\partial G(v_1, v_2, u_1, u_2)}{\partial v_2} \right|_{v_1=u_1, v_2=u_2} \tag{3.1.11}$$

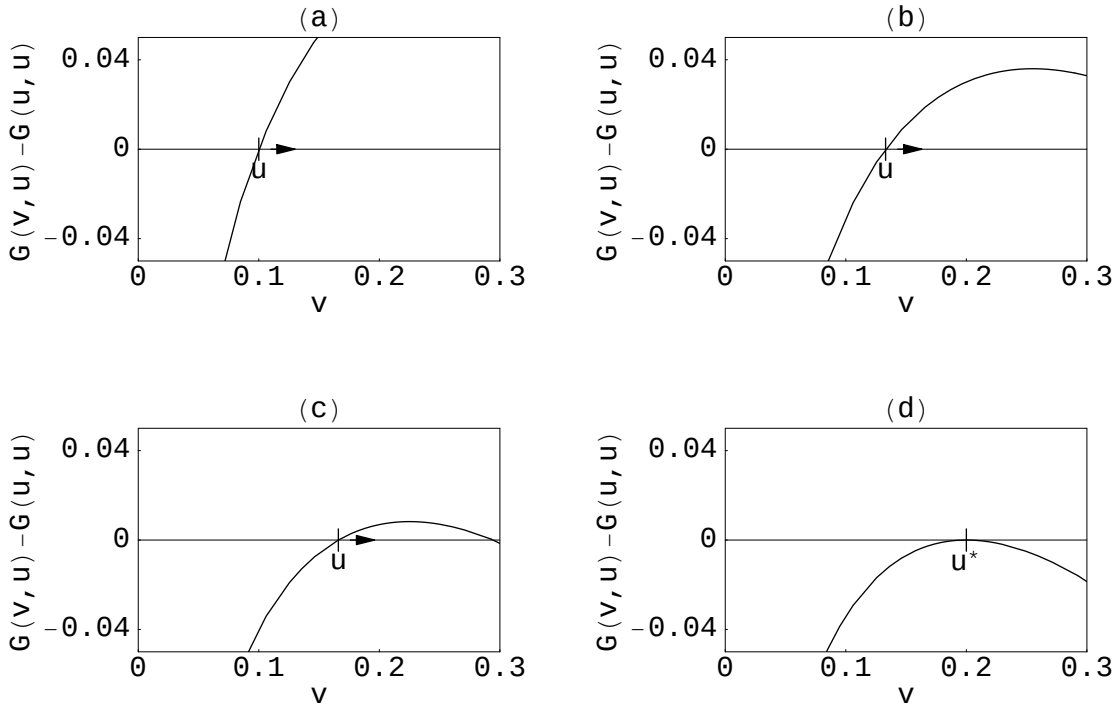

Figure 3.1: Strategy dynamics resulting in an ESS. The curves show the difference in per capita growth rate between a virtual strategy v and the population mean strategy u, $G(v,u) - G(u,u)$. Arrows show the direction of evolution for the population mean strategy u. The temporal order of the plots is (a), (b), (c) then (d). The population strategy u comes to rest at an ESS u^*.

where u_1 and u_2 the mean strategies for each component, v_1 and v_2 are two virtual strategy components, and η_1 and η_2 are the variance of each of the strategy components. Equations (3.1.10) and (3.1.11) are used to test the convergent stability of equilibrium strategies later in the chapter.

3.2 Harmful tactics in mating

Sexual reproduction between males and females is frequently a discordant affair because of a conflict between the interests of males and females. This means that if an adaptation to increase fitness arises in one sex, then a counter-adaptation may arise in the other, leading to a potential, perpetual coevolutionary arms race [54]. In hermaphrodites, these conflicts are further complicated because an individual can take both roles at the same time, while simultaneously making fine adjustments to the resources allocated to each sex [54, 55].

There has been some debate as to precise definitions, but the origin and maintenance of harmful male adaptations is generally understood from two main perspectives. First, the 'adaptive harm' hypothesis [56–58]; defines a general scenario in which a male harming a female causes a change in behaviour so as to directly increase paternity (e.g. reduced probability of re-mating). An alternative perspective is that of 'collateral harm', where harm evolves as a negative pleiotropic side effect of a trait that benefits the male function [59], such as increased efficiency of sperm displacement.

Examples of male harming behaviour include the seminal 'toxins' of Droso-

phila fruitflies [60], genital spines that prolong copulation [61], hypodermic insemination to moderate female choice [62], and 'love' darts to hormonally influence fertilisation [63, 64]. The aim of all these tactics appears to be to increase the sperm precedence of the harming male, though the tactics also appear to cause physical damage to the female. In extreme circumstances, some tactics have been observed to increase probability of death of females following mating [65, 66].

It has been shown [67] that collateral harm may evolve in both gonochorists and hermaphrodites when linked to sperm precedence. However their model was limited in that individuals could not mate more than twice, and resource allocation between male and female functions was fixed for hermaphrodites. As previous models of sperm competition in hermaphrodites [68, 69] have shown that the most successful resource allocation strategy is often not an equal division of resources between male and female functions, then further refinements are clearly required.

Here a previous sperm competition model is extended [68, 69] to include mating tactics which cause collateral harm. These tactics increase sperm precedence for the sperm donor but reduce the survival probability of the sperm recipient. Fitness equations are formulated analytically and solved numerically to find evolutionary stable pairs of values for resource allocation to male function and degree of harmful mating tactics. This mathematical approach allows predictions which would be difficult to obtain simply by intuition.

3.3 Sperm competition models

3.3.1 Charnov's Infinity Model

Charnov [68] considered a hermaphrodite over an interval of time yielding one mating. Each hermaphrodite has a total resource R at its disposal per mating. This resource is divided such that a fraction r is allocated to the male function (sperm production) leaving a fraction, $(1-r)$, to the female function (egg production). Sperm competition is modelled by a function $\phi(r)$ which represents the fraction of sperm an individual displaces in its mating partner's sperm store. Charnov [68] considered a mutant X with resource allocation $\hat{r}$ in a population in which all individuals have resource allocation r. Upon mating the mutant displaces a fraction of sperm, $\phi(\hat{r})$, in the stores of its partner, Y. When Y next lays eggs, X fathers a fraction $\phi(\hat{r})$. Y goes on to mate again, almost certainly with a wild type, as the mutant is rare. This latest mate displaces a fraction $\phi(r)$ of Y's sperm stores, leaving a fraction $[1-\phi(r)]$ from previous mates. When Y lays again, X fathers an additional fraction $\phi(\hat{r})[1-\phi(r)]$. This process continues as Y re-mates an infinite number of times. Thus, the fitness of this mutant, X, from one mating is given by,

$$W^{(CM)} = R(1-\hat{r}) + R(1-r)\phi(\hat{r})\left[1 + [1-\phi(r)] + [1-\phi(r)]^2 + \ldots\right]. \tag{3.3.1}$$

The first term in equation (3.3.1) represents the fitness from the mutant's female function and the second term represents fitness from the mutant's male function. Equation (3.3.1) can be summed as a geometric series and the ESS for

resource allocation calculated.

Charnov [68] tested three different sperm displacement functions, $\phi(r)$, and found that the exact form of the sperm displacement function did not affect the ESS for resource allocation. The sperm displacement functions used by Charnov were characterised by the parameter,

$$\delta = Rc/\mu, \tag{3.3.2}$$

where c is a constant which converts resource to the number of sperm deposited in the recipient's sperm stores and μ is the total sperm remaining in the recipients sperm stores from previous mating partners.

One sperm displacement function considered by Charnov [68] was the case where new sperm is mixed with the stored sperm and a fair sample of this mixture is stored, $\phi_1(r) = \delta r/(\delta r + 1)$. Another sperm displacement function considered by Charnov [68] represents the case in which sperm flows smoothly into the sperm stores with constant mixing and flushing of new and old sperm, $\phi_2(r) = 1 - e^{-\delta r}$. The sperm stored from previous mating partners (μ) was assumed to be constant in the investigations of Charnov [68] and a modified version of Charnov's model by Greeff and Michiels [69]. This is also assumed in the harmful mating model constructed later in this chapter.

3.3.2 Finite Number of Matings Model

Greeff and Michiels [69] modified the model of Charnov [68] by considering a hermaphrodite which took part in T reproductive bouts. It was assumed that

the population had non-overlapping generations and reproductive bouts were synchronous across the population. Following Charnov [68], their model assumed that an individual oviposits after each mating and that resource allocation is fixed for an individual's lifetime. Lifetime reproductive success (the total number of offspring produced) was used as a measure of fitness.

Greeff and Michiels [69] considered a mutant with resource allocation $\hat{r}$ in a population with resource allocation r. The mutant's fitness from female function is $TR(1-\hat{r})$. The fitness from the mutant's male function is given by,

$$w_m^{(GM)} = R(1-r)\phi(\hat{r}) \begin{pmatrix} 1 + [1-\phi(r)] + [1-\phi(r)]^2 + \ldots + [1-\phi(r)]^{T-1} + \\ 1 + [1-\phi(r)] + [1-\phi(r)]^2 + \ldots + [1-\phi(r)]^{T-2} + \\ \vdots \\ 1 \end{pmatrix}. \tag{3.3.3}$$

The large brackets in equation 3.3.1 do not infer a matrix, they contain a long sum of terms where separate lines are used to aid in understanding. Starting with the first mating, each next line in equation (3.3.3) represents male fitness achieved through each successive mating by the mutant. Equation (3.3.3) can be summed as a geometric series. Greeff and Michiels [69] found the ESS resource allocation by numerically searching for a strategy which cannot be invaded by mutants. For simplicity Greeff and Michiels [69], like Charnov [68] before them, used the approximation that the sperm storage organ already contains sperm at the first mating. They pointed out that this approximation should become more accurate with increasing T.

In agreement with Charnov [68], Greeff and Michiels [69] found that sperm displacement functions $\phi_1(r)$ and $\phi_2(r)$ gave similar results in their analysis. However, they found that $\phi_1(r)$ often yielded equations solvable using standard analytical techniques and used $\phi_1(r)$ in their model.

3.4 Harmful mating model

Here the sperm competition model by Greeff and Michiels [69] is extended to include a harmful mating tactic which promotes the sperm precedence of the sperm donor at the expense of the sperm recipient. It was found that sperm displacement functions $\phi_1(r)$ and $\phi_2(r)$ gave similar results in the analysis of our model. However, $\phi_1(r)$ yielded equations which were much simpler to solve thus the sperm displacement function, $\phi_1(r) = \delta r/(\delta r + 1)$ has been used as a basis in the model described below.

A tactic which increases the sperm precedence of the donor should increase the total fraction of sperm that an individual can displace in the sperm stores of the recipient. This increase is characterised using the parameter s, where the sperm displacement function becomes,

$$\phi(r, s) = \frac{r(\delta + s)}{r(\delta + s) + 1}. \tag{3.4.1}$$

An hermaphrodite with larger value of s will displace more sperm and thus father more offspring. An s value of 0 returns ϕ to the Charnov [68] formulation. The additive relation between δ and s proposed in equation (3.4.1) is the simplest form that captures this interaction. For example, a multiplicative re-

lationship would be reasonable for the large δ and s limit but not for, $\delta \to 0$, which corresponds to no sperm displacement.

Our model considers the case where harm to the sperm recipient is a side effect of a tactic which promotes a donor's sperm. An example of this in nature is the increased probability of death of females following mating [65, 66]. In our model, when a harmful mating tactic is employed by a sperm donor there is an associated probability of death for the sperm recipient. This possible death occurs between mating and laying eggs.

When harmful mating tactics are not used, $s = 0$, the probability of survival of a sperm recipient is unity. It is expected that an increase in the ability to displace sperm using a harmful mating tactic, s, should result in reduced probability of survival for the sperm recipient. The probability of survival, $\sigma(s)$, is a decreasing function of s. An appropriate function relating the survival probability of sperm recipient to parameter s was selected to be,

$$\sigma(s) = \left(\frac{1}{1+s}\right)^m. \tag{3.4.2}$$

The relationship between survival probability and s is tuned by a severity parameter m. Increasing m increases the probability of death, for any given value of $s > 0$ (see figure 3.2). m therefore characterises the severity of the harmful mating tactic, with larger m corresponding to greater severity. An example of this is the acceleration of harm with respect to increased dose observed for a number of different toxins [70, 71]. We chose equation (3.4.2) for mathematical convenience but our results below do not depend on the precise form of the survival probability.

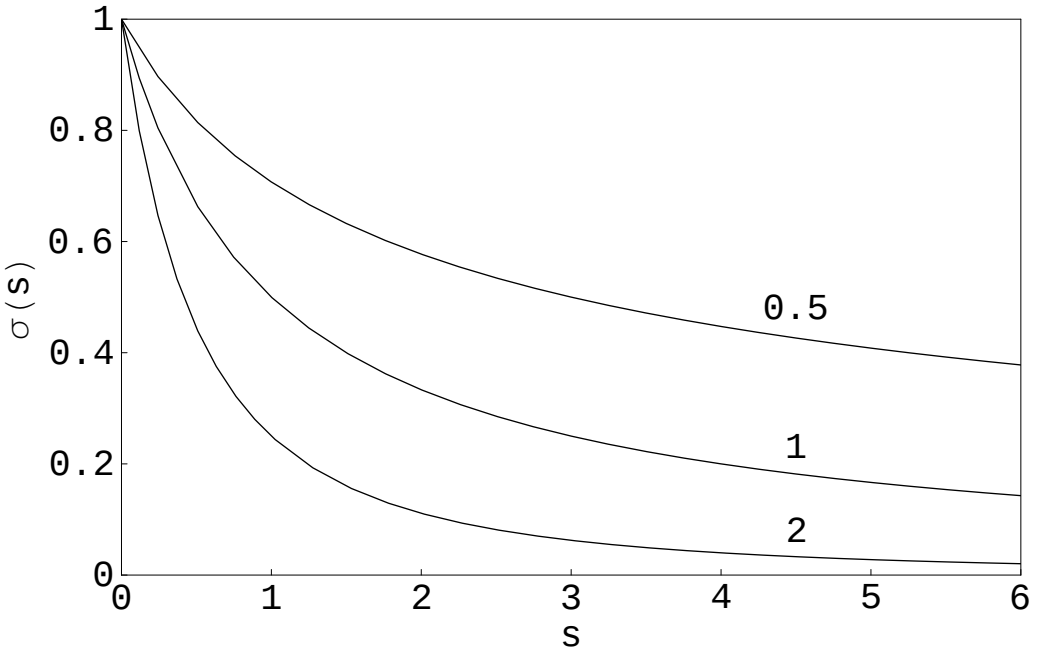

Figure 3.2: Survival probability of sperm recipient, σ, versus s. Plots are shown for the severity parameter $m = 0.5$, 1 and 2.

A hermaphrodite's life in our model proceeds in the following way: it mates in both male and female function, it experiences a probability of death due to harm it received during mating, and if the hermaphrodite survives it lays eggs. This cycle is repeated a maximum of T times. Consider a rare mutant using the strategy $(\hat{r}, \hat{s})$ in a population using the strategy (r, s). If the maximum number of matings, $T = 2$, the fitness of the rare mutant due to its female function is given by,

$$w_f(\hat{r}, \hat{s}, r, s) = \sigma(1 - \hat{r})R + \sigma^2(1 - \hat{r})R. \tag{3.4.3}$$

For ease of notation the survival probabilities are written, $\hat{\sigma} = \sigma(\hat{s})$ and $\sigma = \sigma(s)$. The first term in equation (3.4.3) is the product of the probability that the mutant survives the first mating with a wild type to lay eggs and the resource

the mutant has allocated to egg production. The second term is the product of the probability that the mutant survives the first and second matings with wild types to lay a second clutch of eggs and the resource the female has allocated to egg production.

The fitness from the female function of a rare mutant hermaphrodite using strategy $(\hat{r}, \hat{s})$ in a population with strategy (r, s) is generalised for T matings by the equation,

$$w_f(\hat{r}, \hat{s}, r, s) = R(1 - \hat{r}) \sum_{i=1}^{T} \sigma^i. \tag{3.4.4}$$

The fitness of the same mutant due to its male function, for $T = 2$, is given by,

$$w_m(\hat{r}, \hat{s}, r, s) = \begin{pmatrix} \hat{\sigma}\hat{\phi}R(1-r) + \hat{\sigma}\sigma\hat{\phi}\,(1-\phi)\,R(1-r) + \\ \sigma\hat{\sigma}\hat{\phi}R(1-r) \end{pmatrix}, \tag{3.4.5}$$

where $\hat{\phi} = \phi(\hat{r}, \hat{s})$ and $\phi = \phi(r, s)$. The first term in equation (3.4.5) is from eggs produced by the sperm recipient (wild type) immediately after mating with the mutant. This is a product of the probability that the wild type survives the mating, the fraction of sperm the mutant displaces in the wild type's sperm stores and the number of eggs produced by the wild type. The second term in equation (3.4.5) is from offspring produced by the wild type after it engages in a second mating with another wild type. Thus in order to lay eggs the wild type needs to have survived its first and second matings. The second mating will leave a fraction $\phi(\hat{r})\,(1 - \phi(r))$ of the mutants sperm in the wild type's sperm stores. The third term in equation (3.4.5) is from the second mating of the mutant. The mutant needs to have survived its first mating in female function in order to engage in a second mating. Thus the third term is equal to the

first term multiplied by the probability that the mutant lives to mate a second time. Following the models of Charnov [68] and Greeff and Michiels [69] it is approximated that there is sperm stored at the first mating. This approximation should be accurate for large numbers of matings or large values of δ, where mating with an individual with no sperm stored becomes less significant. For small number of matings and small δ the approximation becomes less accurate, the impact of this is discussed later.

The fitness from the male function of a rare mutant using strategy $(\hat{r}, \hat{s})$ in a population using strategy (r, s) is generalised for T matings by the equation,

$$w_m(\hat{r}, \hat{s}, r, s) = R(1-r)\hat{\phi}\hat{\sigma} \sum_{i=1}^{T} \left(\sigma^{i-1} \sum_{j=0}^{T-i} \sigma^j \left(1-\phi\right)^j \right). \tag{3.4.6}$$

The second sum in equation (3.4.6) is over the mutant's mating partner going on to mate $(T-i)$ times with others in the population, weighted by the probability that the mating partner survives to take part in the jth mating, where $j > i$. The first sum in equation (3.4.6) sums the T matings of the rare mutant in question, weighted by the probability that the mutant survives to take part in the ith mating. Equation (3.4.6) can be summed as a geometric series.

Notice that in equations (3.4.4) and (3.4.6), fertilised egg production is not limited by ability to get sperm, but by resource allocated to eggs. Also, male reproductive success is limited by ability to gain access to eggs (these are the assumptions behind Bateman's principle [53, 72]). A consequence of these assumptions is that, if there is no competing sperm, males can fertilise eggs with vanishingly small amounts of sperm. Under these conditions, this can act as a selection pressure for unrealistically low allocation to male function. This as-

sumption was also used by Charnov [68] and Greeff and Michiels [69].

The total fitness $W(\hat{r}, \hat{s}, r, s)$ of a mutant individual using strategy $(\hat{r}, \hat{s})$ in a population using strategy (r, s) is given by the sum of its fitness from male function and female function (equations (3.4.4) and (3.4.6)), $W = w_f + w_m$.

ESS and convergent stability were tested using the methods described above in section 3.1. The G-function describing the evolution of the harmful mating model described above can be written,

$$G(\hat{r}, \hat{s}, r, s) = W(\hat{r}, \hat{s}, r, s) - 1, \tag{3.4.7}$$

where $\hat{r}$ and $\hat{s}$ represent virtual strategies and the -1 term is due to parallel update mechanism of the model; *i. e.* the daughter population is derived from parent population with no overlapping of generations.

3.5 Stability Analysis

Equilibrium strategies were determined by solving equations (3.5.1) and (3.5.2) simultaneously subject to the constraints $0 \leq r \leq 1$ and $s \geq 0$. These equations were solved numerically using Mathematica.

$$\left.\frac{\partial G(\hat{r}, \hat{s}, r, s)}{\partial \hat{r}}\right|_{\hat{s}=s, \hat{r}=r} = 0 \tag{3.5.1}$$

$$\left.\frac{\partial G(\hat{r}, \hat{s}, r, s)}{\partial \hat{s}}\right|_{\hat{s}=s, \hat{r}=r} = 0 \tag{3.5.2}$$

3.5.1 Interior ESS

An equilibrium is an ESS if $G(\hat{r}, \hat{s}, r^*, s^*) < G(r^*, s^*, r^*, s^*)$. This can be tested by performing a Taylor expansion about the equilibrium,

$$\delta G \equiv G(\hat{r}, \hat{s}, r^*, s^*) - G(r^*, s^*, r^*, s^*)$$

$$\delta r \left[\frac{\partial G}{\partial \hat{r}}\right]_* + \delta s \left[\frac{\partial G}{\partial \hat{s}}\right]_* + \frac{1}{2}\left[(\delta r)^2 \frac{\partial^2 G}{\partial \hat{r}^2} + (\delta s)^2 \frac{\partial^2 G}{\partial \hat{s}^2} + 2\delta r \delta s \frac{\partial^2 G}{\partial \hat{r} \partial \hat{s}}\right]_* + \ldots \tag{3.5.3}$$

where $\delta r = \hat{r} - r^*$, $\delta s = \hat{s} - s^*$. The notation $[\ \ ]_*$ denotes that all derivatives are evaluated at $\hat{r} = r = r^*, \hat{s} = s = s^*$. The first two terms on the right-hand side of equation (3.5.3) are zero by equilibrium conditions. Equation (3.5.3) can then be arranged in matrix form, and eigenvalues calculated. A strategy is an ESS if eigenvalues are negative. All interior equilibria that were calculated for the harmful mating model were ESSs.

3.5.2 Boundary ESS

The following will consider the lower boundary value for the strategy component s as an example ($s = 0$), however similar reasoning (not shown) was used to test the stability of the boundary values for the strategy component r ($r = 0$ and $r = 1$). For this case ($s = 0$), boundary equilibria can be calculated by solving the equilibrium equation (3.5.1) with $s = 0$. On substituting the equilibrium value for r and $s = 0$ into the Taylor expansion in equation (3.5.3), the δr term (first term) in equation (3.5.3) is zero due to the equilibrium condition and the

δs term (second term) dominates. As the lower boundary value for s is being considered it follows that, $\delta s > 0$, hence a boundary ESS must satisfy,

$$\left[\frac{\partial G}{\partial \hat{s}}\right]_* < 0 \tag{3.5.4}$$

and,

$$\left[\frac{\partial^2 G}{\partial \hat{r}^2}\right]_* < 0. \tag{3.5.5}$$

Some boundary equilibria for the harmful mating model were ESS some were not, this is discussed later.

3.5.3 Interior convergent stability

Local convergent stability is tested by dispacing the population away from the equilibrium, (r^*, s^*), then testing if the population would evolve back to the equilibrium via the strategy dynamics given in equations (3.1.10) and (3.1.11). This is tested by performing a Taylor expansion of the strategy dynamical equations about (r^*, s^*),

$$\left[\frac{\partial G}{d\hat{r}}\right]_\dagger = \left[\frac{\partial G}{\partial \hat{r}} + \delta r\left(\frac{\partial}{\partial \hat{r}} + \frac{\partial}{\partial r}\right)\frac{\partial G}{\partial \hat{r}} + \delta s\left(\frac{\partial}{\partial \hat{s}} + \frac{\partial}{\partial s}\right)\frac{\partial G}{\partial \hat{r}}\right]_*, \tag{3.5.6}$$

$$\left[\frac{\partial G}{d\hat{s}}\right]_\dagger = \left[\frac{\partial G}{\partial \hat{s}} + \delta r\left(\frac{\partial}{\partial \hat{r}} + \frac{\partial}{\partial r}\right)\frac{\partial G}{\partial \hat{s}} + \delta s\left(\frac{\partial}{\partial \hat{s}} + \frac{\partial}{\partial s}\right)\frac{\partial G}{\partial \hat{s}}\right]_*, \tag{3.5.7}$$

where $\delta r = (\hat{r} - r^*) = (r - r^*)$, $\delta s = (\hat{s} - s^*) = (s - s^*)$, and the $\dagger$ indicates that the derivative is evaluated at, $(\hat{r} = r = r^* + \delta r, \hat{s} = s = s^* + \delta s)$. The first terms in equations (3.5.6) and (3.5.7) are equal to zero by equilibrium conditions. Equations (3.5.6) and (3.5.7) can then be written in matrix form and convergent stability tested by eigenvalue analysis. Negative eigenvalues indicate convergent stability.

All interior equilibrium that were calculated for the harmful mating model displayed convergent stability as well as being ESSs.

3.5.4 Boundary convergent stability

The following will consider the lower boundary value for the strategy component s as an example ($s = 0$), however similar reasoning (not shown) was used to test the stability of the boundary values for the strategy component r ($r = 0$ and $r = 1$). For this case ($s = 0$), boundary equilibria can be calculated by solving the equilibrium equation (3.5.1) with $s = 0$. On substituting the equilibrium value of r and $s = 0$ into the Taylor expansions in equations (3.5.6) and (3.5.7), the first term on the right hand side of equation (3.5.6) goes to zero due to the equilibrium condition.

Perturbations away from the lower boundary value of s can only be positive, thus the equilibrium shows convergent stability if,

$$\left[\frac{\partial G}{\partial \hat{s}}\right]_* < 0 \tag{3.5.8}$$

and,

$$\left[\left(\frac{\partial}{\partial \hat{r}} + \frac{\partial}{\partial r}\right)\frac{\partial G}{\partial \hat{r}}\right]_* < 0. \tag{3.5.9}$$

Some boundary equilibria for the harmful mating model demonstrated convergent stability some did not. Though all boundary equilibria which were ESSs also demonstrated convergent stability and all boundary equilibria that were not ESS did not demonstrate convergent stability. Thus, for the parameters tested the harmful mating model only displays CSS and invasible repellor

points (see table 1.3).

3.6 Results and Discussion

The stability of harmful mating tactics was investigated by varying the parameters T (number of matings), δ (a measure of ability to displace sperm without harmful mating tactic, see equation (3.3.2)) and m (severity of harmful mating tactic). Analysis showed three possible outcomes; not using harmful mating tactics is the ESS, using harmful mating tactics is the ESS and no viable ESS. A phase diagram for the outcomes (for constant T) is plotted in figure 3.3.

In the region of figure 3.3 marked 'no harm', there is a unique boundary ESS $(r^* > 0, s^* = 0)$ that also shows convergent stability. Harmful mating tactics cannot evolve in this region. In the region of figure 3.3 marked 'harm', boundary points ($s = 0$) are not an ESS, however there exists a unique ESS, $(r^* > 0, s^* > 0)$, which shows convergent stability. In this region, rare mutants that use harmful mating tactics will always invade a resident population where harm is absent. One possible biological consequence of these inferences is that polymorphism for 'harm'/'no harm' is an unstable condition, and so will tend not to persist.

Following mating with an individual using the ESS, s^*, the probability an individual survives, $\sigma(s^*)$, can be found by substituting the ESS s^* and the model parameter m into equation (3.4.2). Figure 3.4 plots the survival probability per mating in a population using the ESS, $\sigma(s^*)$, as a function of the model parame-

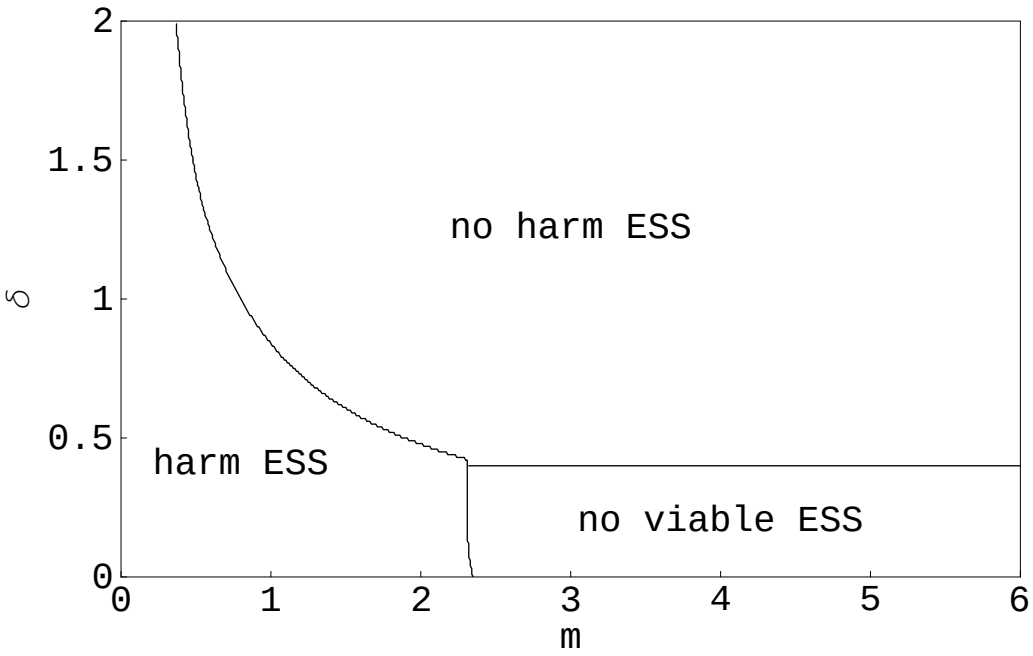

Figure 3.3: For number of matings $T = 4$, this figure shows the ESS phase diagram for parameters m, severity of harmful mating tactic, and δ. In the region marked 'no harm', not using harmful mating tactics is the ESS. In the region marked 'harm', using harmful mating tactics is the ESS. In the region marked 'no viable ESS' $r^* \to 0$ so sperm competition ceases.

ter δ for two different values of T (the parameter denoting the maximum number of matings) and $m = 1$. The survival probability is unity when 'no harm' is an ESS ($s^* = 0$). When $\delta \sim 0.8$, there are discontinuities in the curves and survival probability drops rapidly. This is because the use of a harmful mating tactic ($s^* > 0$) is now an ESS (see figure 3.3 at $m = 1$). As δ decreases, a hermaphrodite's ability to displace sperm without the use of the harmful mating tactic decreases. It then becomes necessary for a hermaphrodite to escalate the use of the harmful mating tactic to increase sperm displacement. This occurs at the expense of its mating partner's probability of survival. An interesting outcome is that the parameter T has little effect on the ESS level of harmful mating tactic, s^*, possibly because the mean lifespan, given by $(1 - \sigma(s))^{-1}$, doesn't allow most individuals to complete T matings when harmful mating tactics are present.

For finite numbers of matings Greeff and Michiels [69] observed that decreasing δ resulted in an increased resource allocation to male function r^*. They noticed an exception for small δ and T, when $r^* \to 0$. This was attributed to the poor ability to displace rival sperm from the receiver's sperm storage organ. The ESS resource allocation (r^*) from our analysis is plotted as a function of δ in figure 3.5. A discontinuity is again observed at value of $\delta \sim 0.8$ and coincides with s^* becoming greater than zero. It was observed that as δ tends to zero the ESS resource allocation for $T > 2$ converges. This coincides with similar values of s^* for different T, and the mean lifespan of individuals becoming shorter than that required to complete T matings.

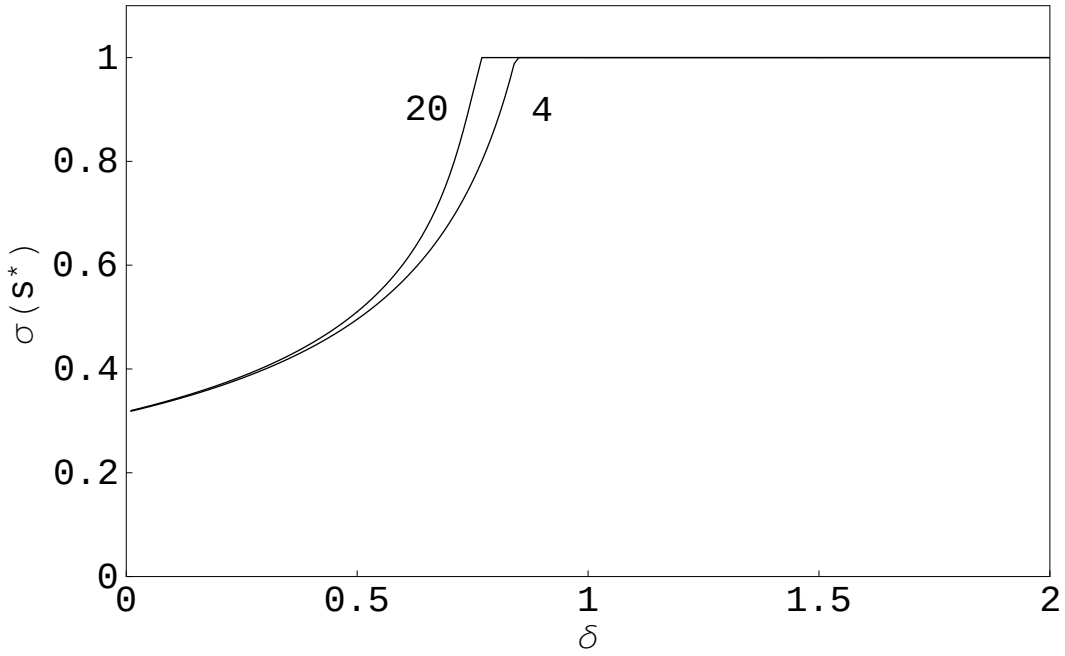

Figure 3.4: Survival probability in a population using the ESS level of harm, $\sigma(s^*)$, versus δ. Plots shown for number of matings, $T = 4$ and 20. The severity parameter $m = 1$, for both plots.

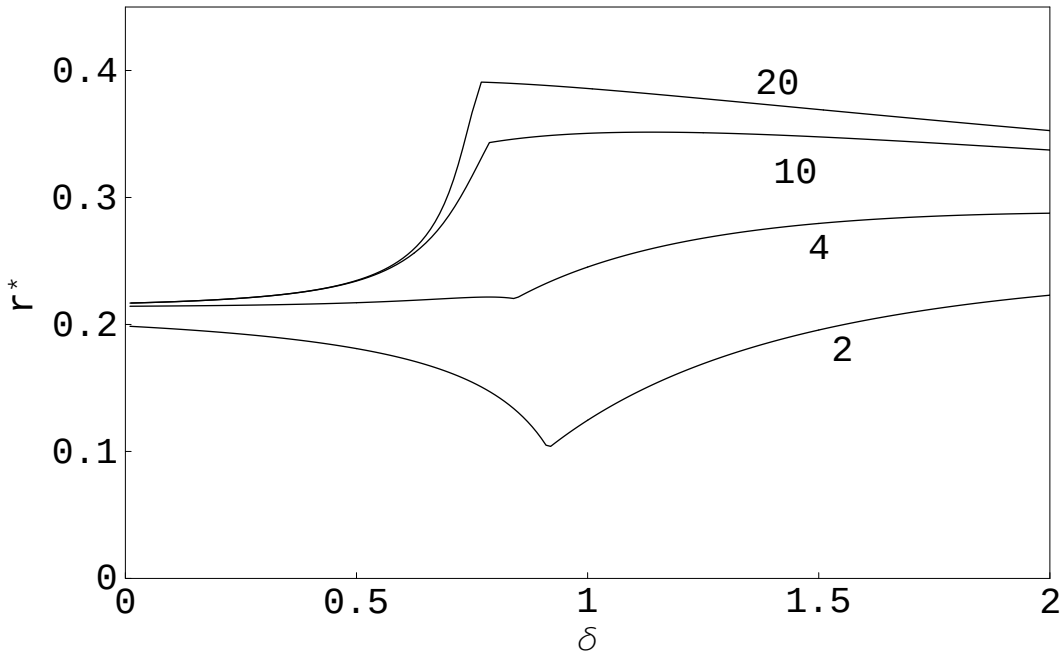

Figure 3.5: ESS resource allocation, r^*, versus δ. Plots shown for number of matings, $T = 2$, 4, 10 and 20. The severity parameter $m = 1$, for all plots.

Figure 3.5 shows that harmful mating tactics should lead to a distinctly female biased resource allocation strategy, contrasting markedly with the conclusions of Greeff and Michiels [69], who found that for large number of matings T and small δ, the resources allocated between male and female function tend to approach equality ($r^* \to 0.5$). One of the main conclusions of their paper may therefore only apply to hermaphrodites where harmful mating tactics are absent. This contrast can be understood by looking at what happens to the ability to displace sperm, measured by $(\delta + s^*)$, when the use of harmful mating tactics becomes stable. Once the use of harmful mating tactics become stable, decreasing the parameter δ actually results in an increase in the potential amount of

sperm which can be displaced, $(\delta + s^*)$. The intuitive explanation for this is that if sperm displacement is made more efficient by harmful mating tactics, then the ESS returns to a more female biased resource allocation strategy. In addition, increased mortality rates due to harmful mating should reduce r^*, as mortality decreases the return from male function [68].

Calculating the sperm displacement function $\phi(\delta, r^*, s^*)$, from the ESS values r^* and s^* for a given set of model parameters (δ, T, m), gives the fraction of offspring fathered by the last male mating partner. Close to the boundary between 'harm' and 'no harm' in Figure 3.3, $\phi\,(\delta, r^*, s^*)$ is typically around 0.1 to 0.3, marking the largest values for which harmful mating can invade a population. Deep inside the region where harmful mating tactics are an ESS (small m, small δ), $\phi\,(\delta, r^*, s^*)$ increased to values of 0.3 to 0.6. This may therefore indicate that harmful mating tactics are likely to initially evolve in populations where the first mate gains most fertilisation, but can lead to last male sperm precedence. Decreasing the severity parameter of the harmful mating tactic (decreasing m), was found to have a marked impact on sperm displacement, following the invasion of harmful mating tactics (Figure 3.6). In comparison the parameter T was found to have a very small effect, with large T resulting in larger values of $\phi\,(\delta, r^*, s^*)$ (not shown). This is a result of r^* and s^* not varying much with T, as explained above.

If ability to displace sperm in a partner is low, $(\delta + s)$ is small, many future laying events are required by a sperm donor's partner to compensate for

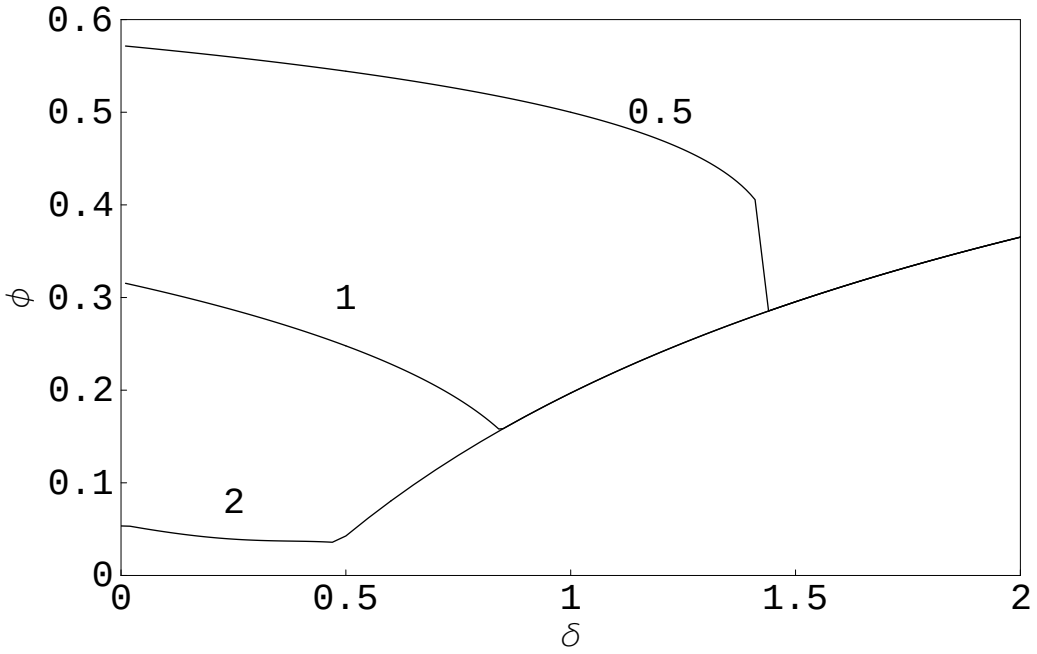

Figure 3.6: ESS sperm displacement, $\phi(\delta, r^*, s^*)$, versus δ. Plots shown for the severity parameter of harmful mating tactic; $m = 0.5$, 1 and 2. Number of matings $T = 4$, for all plots.

this high investment, otherwise investment in the female function would yield higher fitness. However, if the subsequent number of laying events isn't sufficient to make investment in the male function profitable, the ESS for resource allocation to male function can tend to zero. If this occurs then it follows that $\phi(\delta, r^*, s^*)$ tends to zero, thus sperm competition ceases. This unrealistically low allocation to male function is a consequence of the approximations used in constructing our model. When displacing rival sperm is difficult (δ is small) and the number of matings is small, fitness due to mating with an individual with no sperm stored should become more significant. Our model approximates there to be sperm stored at the first mating and that production of fertilised eggs is not limited by the availability of sperm. Thus, when T and $(\delta + s)$ are both small the individual is better off investing all in female function and $r^* \to 0$. This marks the limit in the validity of our approximations.

The ESS is for no resource allocated to the male function ($r^* \to 0$) on the boundary of the 'no viable ESS' region (figure 3.3) and is equal to zero inside this region. This is because the return in paternity due to a finite number of matings, T, is insufficient and a hermaphrodite is better off investing all in female function. Increasing T shifts the boundary of the 'no viable ESS' region in Figure 3.3 to lower values of δ and higher values of m. In the limit that T tends to infinity the 'no viable ESS' region disappears for a plot equivalent to figure 3.3. $r^* \to 0$ was also observed by Greeff and Michiels [69]. They observed that for finite T, resource allocation to male function tends to zero for small δ and small T. In the limit that T tends to infinity r^* tends to 0.5 for small δ [68].

The fitness of a population using a particular ESS strategy (r^*, s^*) can be calculated by substituting, $\hat{r} = r = r^*$ and $\hat{s} = s = s^*$, into the equation for total fitness, W. This gives the fitness in units of the resource available per individual per mating, R. If a species is competing with other species for the same resource under density dependent selection, then the growth rate of each will ultimately determine success or extinction.

Our model assumes the number of eggs to be the limiting factor in population growth, thus greater allocation to female function would be expected to increase the fitness of the population. Perhaps surprisingly, the model instead shows that harmful mating tactics more than compensate. Thus, although resource allocation may be female biased, this heavy bias makes little difference to the overall fitness of a population once harm invades, especially when δ is small, or similarly, when the severity parameter for the harmful mating tactic is low ($m < 0.5$) (Figure 3.7). Nonetheless, the fitness per mating when harm is present is considerably less than when harm is absent (Figure 3.7). In consequence, species that compete under density dependent selection may be at a disadvantage when harmful mating tactics are present.

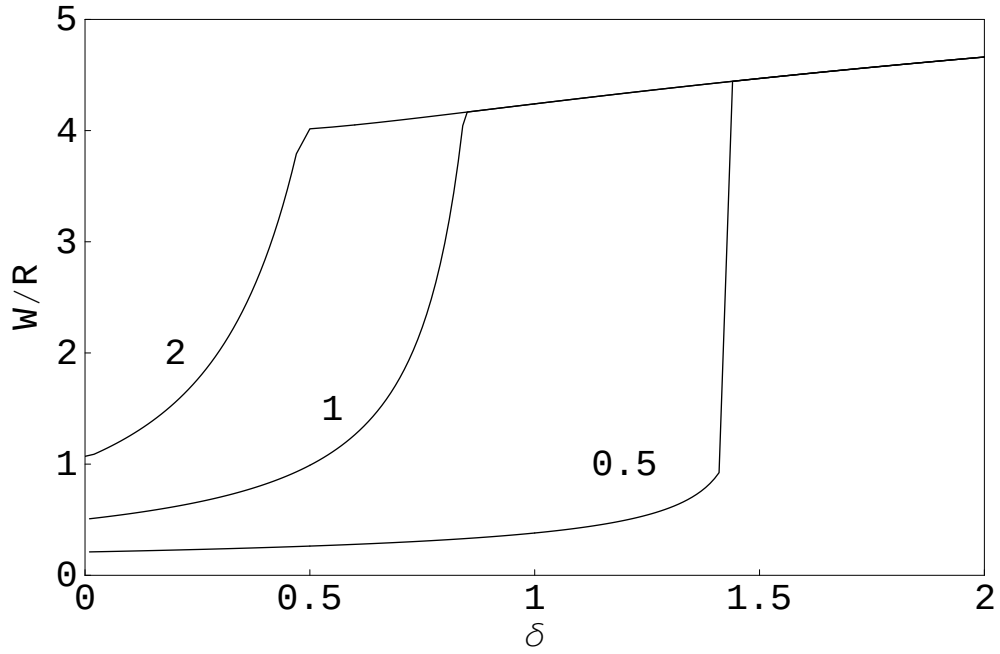

Figure 3.7: Fitness (W) calculated for resident population at ESS, (r^*, s^*) versus δ. Fitness is in units of resource per mating, R. Plots shown for severity parameter of harmful mating tactic, $m = 0.5$, 1 and 2. Number of matings $T = 4$, for all plots.

3.7 Conclusions and future investigations

The majority of the inferences from the harmful mating model are reassuring in that they are in keeping with what might be expected based on intuition. It was found that harmful mating in hermaphrodites is likely to be associated with species in which sperm precedence strongly favours the first mate. Our model predicts that this criterion becomes less important as harmful mating tactics become more efficient. This was explicitly pointed out by [54, 56]. Harmful mating tactics enable the sperm donor to increase its sperm precedence, and can lead to last male sperm precedence for very efficient harmful mating tactics.

In contrast to the conclusions of previous work that did not include harmful mating [69], the model indicates that when harm is also considered, hermaphrodites may again return to a female biased resource allocation strategy, partly because sperm displacement is made more efficient by harmful tactics. Perhaps the most surprising inference is that harmful mating tactics more than compensate in these circumstances, so leading to a reduced fitness. Hermaphrodites that use harmful mating tactics may therefore be at a disadvantage when competing with other species for a limited resource.

The game theoretical approach used in this chapter also provides a useful example of modelling the coevolution of traits. There are many empirical studies of traits that coevolve in natural populations, however, game theoretical models which analyse the coevolution of multiple traits (using vector strategies) are comparatively rare. Similar techniques to those used in this chapter

could be applied to other coevolutionary traits.

CHAPTER 4

Sustainability of Dioecious and Hermaphrodite Populations on a Lattice

4.1 Introduction

Dioecy describes sexually reproducing plant species in which there are two distinct sexes, male and female. One individual of each sex is required for reproduction. The equivalent mating system in animal species is referred to as gonochorism. In contrast to dioecy and gonochorism, simultaneous hermaphrodites have the ability to reproduce in female and male roles simultaneously.

The Allee effect describes a positive relationship between individual fitness and the density of conspecifics (members of the same species) [73]. By far, the most cited cause of the Allee effect is the difficulty of finding mates in sexually

reproducing species [74]. The most typical single-sex (hermaphrodite) model of the Allee effect [75] is represented by,

$$\frac{dh}{dt} = a_1 h(h - a_2)(a_3 - h), \tag{4.1.1}$$

where h is the population density, and a_1, a_2 and a_3 are positive constants ($a_2 < a_3$). Equation (4.1.1) has three equilibria; $h = 0$ and $h = a_3$ are stable, $h = a_2$ is unstable. Below the threshold $h = a_2$ the population converges on $h = 0$, so becomes extinct. Above the threshold $h = a_2$ the population converges on the stable equilibrium, $h = a_3$.

It can be shown that hermaphroditism is a more successful mating strategy than dioecy when the probability of encountering a mate is low. Consider a female in a dioecious population with a one to one ratio of females to males, at each encounter with another individual, the female meets a male with probability $1/2$. In a hermaphrodite population, every encounter of a hermaphrodite would be with a compatible mating partner. All else being equal (encounter rate, number of off-spring produced per mating pair), the hermaphrodite population can reproduce at twice the rate of the dioecious population. This reasoning provides support for the observation that hermaphroditism is often associated with sedentary species, such as plants and animals with poor mate search efficiency [76].

Stochastic spatial models have been extensively applied to chemical, ecological and sociological systems [77, 78]. The Standard Contact Process (SCP) can be used to model populations that reproduce asexually. In the SCP lattice sites can be occupied or vacant. Individuals die at a rate λ and give birth at a rate b.

Offspring are placed on a neighbouring site with probability defined by some displacement kernel.

In the Quadratic Contact Process (QCP) [77], an occupied state becomes vacant at a rate λ, the same as in the SCP. However, in the QCP it takes two particles to make a new one. For this reason the QCP is often referred to as the "sexual reproduction process". A vacant site becomes occupied at a rate $j/4$, where j is the number of diagonally adjacent pairs of occupied neighbours.

The SCP and QCP are often identified as Schlögl's 1st and 2nd models for autocatalytic kinetics, respectively [79]. For the 1st model, $Z \to 2Z$ and $Z \to \oslash$; for the 2nd model, $2Z \to 3Z$ and $Z \to \oslash$, where $Z \to \oslash$ denotes the annihilation of a particle. The mean-field kinetics are quadratic (cubic) for the 1st (2nd) model suggesting a continuous (discontinuous) transition to the absorbing state, $\oslash$. The mean-field kinetics of the QCP can lead to equation (4.1.1).

A special feature of the QCP is that if a population is contained inside a rectangle it can never give birth outside the rectangle [77]. This is because an empty site needs at least two diagonally adjacent nearest neighbours to become occupied. For lattices of finite size, this feature also means that complete columns or rows of empty sites in the lattice cannot become occupied.

To assess the impact of these finite size effects, another spatial model similar to the QCP described above is introduced here and will be referred to as the modified Quadratic Contact Process (MQCP). For the MQCP a hermaphrodite (female) produces offspring with rate proportional to the number of occupied

(male) neighbouring sites. An offspring is placed on a randomly chosen neighbouring site. If the site is empty the offspring takes residence. If the site is occupied the offspring is deleted. This model is based on the sexual reproduction model of Stewart-Cox *et al.* [80] and has the advantage that a population can grow outside a rectangle in which it is contained.

In this chapter, a comparison of the sustainability of hermaphrodite and dioecious populations is presented. Comparisons of the two mating systems are made using the QCP and MQCP simulations along with mean-field analyses of each model.

4.2 Models

All populations reside on a two-dimensional square lattice of side length L, with periodic boundary conditions. For a hermaphrodite population, each lattice site can be occupied by a hermaphrodite (H) or be empty ($\oslash$). For a dioecious population each lattice site can be occupied by a male (M), a female (F) or be empty ($\oslash$). For both mating systems, an occupied state becomes vacant at a rate λ (deathrate).

In the hermaphrodite QCP, a vacant site becomes occupied at rate equal to $j_1 b_1/4$, where j_1 is the number of diagonally adjacent pairs of occupied neighbours and b_1 is the birth rate. Thus, $j_1 = 0$,0,2 and 4 for 0, 1, 3 and 4 occupied nearest neighbour sites respectively. $j_1 = 1$ (0) for two occupied nearest neighbours which are diagonally adjacent (on opposite sides of the vacant site).

In the dioecious QCP, a vacant site becomes occupied at rate equal to $j_2 b_2/4$, where j_2 is the number of compatible diagonally adjacent pairs of occupied neighbours and b_2 is the birthrate. Thus, an (M, M) or (F, F) diagonally adjacent pair does not increment j_2. The gender of the offspring is set to male with probability α and female with probability $(1 - \alpha)$.

In the hermaphrodite MQCP, an occupied site produces an offspring at a rate equal to $k_1 b_3/4$, where k_1 is the number of occupied nearest neighbours and b_3 is the birth rate. A nearest neighbour site is chosen randomly to place the offspring on. If the chosen site is empty the offspring is placed on the site. If the site is occupied the offspring is deleted.

In the dioecious MQCP, a female site produces an offspring at a rate equal to $k_2 b_4/4$, where k_2 is the number of male nearest neighbours and b_4 is the birth rate. A nearest neighbour site is chosen randomly to place the offspring on. If the chosen site is empty the offspring is placed on the site. If the site is occupied the offspring is deleted. The gender of the offspring is set to male with with probability α and female with probability $(1 - \alpha)$.

There exists a subtle difference between the MQCP and QCP. Letting $b_1 = b_2$ in the QCP, a hermaphrodite pair of diagonally adjacent neighbours are capable of producing offspring at the same rate as a male-female pair of diagonally adjacent neighbours. Letting $b_3 = b_4$ in the MQCP, a hermaphrodite pair of nearest neighbours can produce offspring at twice the rate of a male-female pair of nearest neighbours. For example, consider an isolated pair of nearest neighbours, both members of the hermaphrodite pair can produce offspring at

a rate $b_3/4$ where as only the female can produce offspring in the dioecious pair, she does this at a rate $b_4/4$. Thus, the MQCP proposes a fourfold advantage of hermaphrodite over dioecious populations. Letting $b_3 = b_4$, the MQCP proposes that a female and a hermaphrodite can produce offspring at equal rates provided a mating partner is in the vicinity. Depending on the species in question, either assumption may be valid. Fortunately, scaling the reproductive values appropriately can overcome this difference. For example, letting $b_1 = 2b_2$ in the QCP, proposes that females and hermaphrodites produce offspring at the same rate provided a mating partner is available. Letting $b_4 = 2b_3$, proposes that a hermaphrodite pair produce offspring at an equal rate to a male-female pair in the MQCP.

4.3 Mean-field analysis

4.3.1 Hermaphrodite population

The mean-field kinetics for the hermaphrodite population QCP are given by,

$$\frac{dh}{dt} = -\lambda h + b_1 h^2(1-h), \tag{4.3.1}$$

where h is the density of hermaphrodites residing on the lattice. The reader can substitute $b_1 = 3b_3/4$ for a description the the mean-field behaviour in the MQCP hermaphrodite model. Equilibrium points for equation (4.3.1) are plotted in figure 4.1 as a function of b_1/λ. By appropriate scaling of time ($\tau = \lambda t$), the number of parameters in equation (4.3.1) can be reduced to one (b_1/λ) .

Thus, figure 4.1 is unique for a given value of b_1/λ. Two non-trivial equilibria (one node, one repellor) exist for $b_1/\lambda > 4$. We will refer to this as the survival/extinction phase. If the initial population density is below the unstable equilibrium, growth is negative and the population converges on the trivial equilibrium, $h = 0$. If the initial population density is above the unstable equilibrium the population converges on the stable non-trivial equilibrium. Only the trivial equilibrium exists for $b_1/\lambda < 4$, thus extinction of the population always occurs.

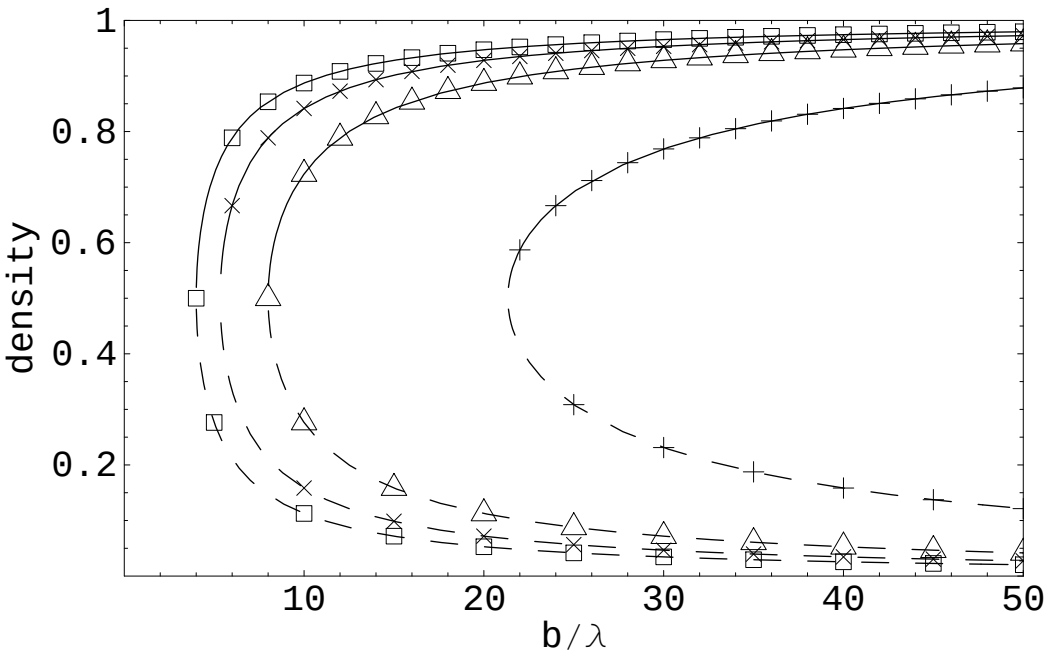

Figure 4.1: Mean-field approximation equilibrium densities for; QCP hermaphrodite (□), QCP dioecious (△), MQCP hermaphrodite (×) and MQCP dioecious (+). The gender ratio of new born offspring $\alpha = 1/2$ for the dioecious populations. Solid (dashed) lines represent stable (unstable) equilibria.

4.3.2 Dioecious population

The mean-field kinetics of the dioecious QCP are given by,

$$\frac{dm}{dt} = -\lambda m + 2b_2 mf(1-m-f)\alpha \tag{4.3.2}$$

$$\frac{df}{dt} = -\lambda f + 2b_2 mf(1-m-f)(1-\alpha) \tag{4.3.3}$$

where m and f are the densities of males and females respectively. The reader can substitute $b_2 = 3b_4/8$ into equations (4.3.2) and (4.3.3) for a description of the the mean-field behaviour for the MQCP dioecious model. Equations (4.3.2) and (4.3.3) have two non-trivial equilibria (one saddle point, one node) for $b_2(1-\alpha)\alpha > 2\lambda$. If the initial population density is sufficiently low, growth is negative and the population converges on the trivial equilibrium, $(m = 0, f = 0)$. If the initial population density is sufficiently high the population converges on the stable non-trivial equilibrium. Typical population dynamics for this system is shown in figure 4.2. Only the trivial equilibrium exists for $b_2(1-\alpha)\alpha < 2\lambda$, thus extinction of the population always occurs.

It has been shown previously [81] that the sex ratio, $\alpha = 1/2$, is the most sustainable. Figure 4.1 shows a comparison of the equilibrium points for the single and dioecious populations with $\alpha = 1/2$. For the dioecious population the equilibrium densities for males and females are summed to demonstrate the size of the total population at equilibrium.

It was explained in the introduction that, if all else is equal, a hermaphrodite population is expected to grow at twice the rate of a dual sex population in the QCP. If we let $b_2 = 2b_1$, the single and dual sex curves in figure 4.1 overlap

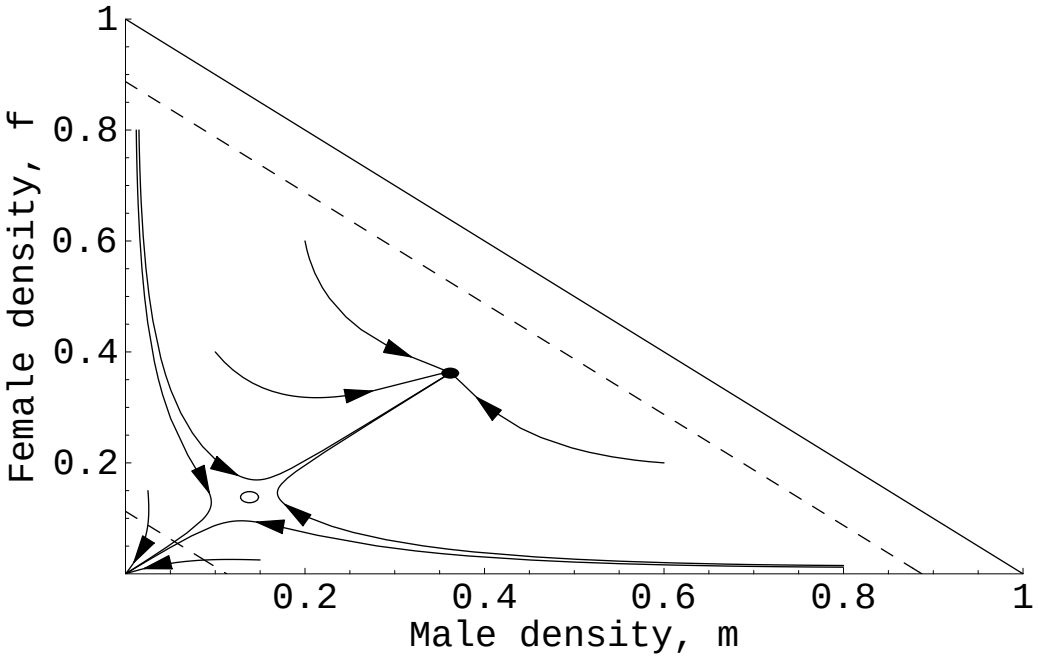

Figure 4.2: Mean-field approximation for QCP: typical dynamics for a population of males and females. Plot shown for $b_2 = 1.0$, $\lambda = 0.1$, $\alpha = 0.5$. Showing the stable equilibrium (filled circle) and unstable equilibrium (empty circle). The dashed lines are a projection of the stable ($m + f \approx 0.85$) and unstable ($m + f \approx 0.1$) equilibria for the hermaphrodite population with the same birth and death rates.

for the QCP. It was also explained in the introduction that the hermaphrodite population can grow at four times the rate of the dioecious population in the MQCP model. If we let $b_4 = 4b_3$, hermaphrodite and dioecious curves in figure 4.1 overlap for the MQCP. As shown by figure 4.2 deviations away from the optimum sex ratio of $1/2$ can hinder the growth of the population. This can have great effect when considering discrete spatial populations with local interactions.

4.4 Results of lattice simulation

Previous simulations [82, 83] have shown that the QCP exhibits a discontinuous phase transition between an active state (finite population) and an absorbing state (extinction). It was also shown that coexistence of stable active and absorbing phases occurs over a finite parameter space. For any parameter set (λ, b) in this coexistence region, "droplets" of the absorbing state embedded in the active cannot grow indefinitely but rather die out, even though the the absorbing state is stable. Similarly, "droplets" of the active state embedded in the absorbing state are short lived.

Figure 4.3 plots population density in the hermaphrodite QCP and MQCP models as a function of b/λ. For each point in the plot the population was initialised with a full lattice and evolved for 10^3 generations. The densities plotted are averaged over the last 10^3 Monte Carlo Steps (MCSs) of the simulation, where 1 MCS = L^2 site selections. A transition from a stable active phase to

a stable absorbing phase occurs at $b_1/\lambda \approx 11$. The location of the QCP transition is in agreement with previous simulations [82, 83] that have shown the coexistence region between $b_1/\lambda \approx 10.5$ and $b_1/\lambda \approx 11.5$ for the QCP. As all simulations in figure 4.3 were initialised with a fully populated lattice only the stable active state of the coexistence region was observed.

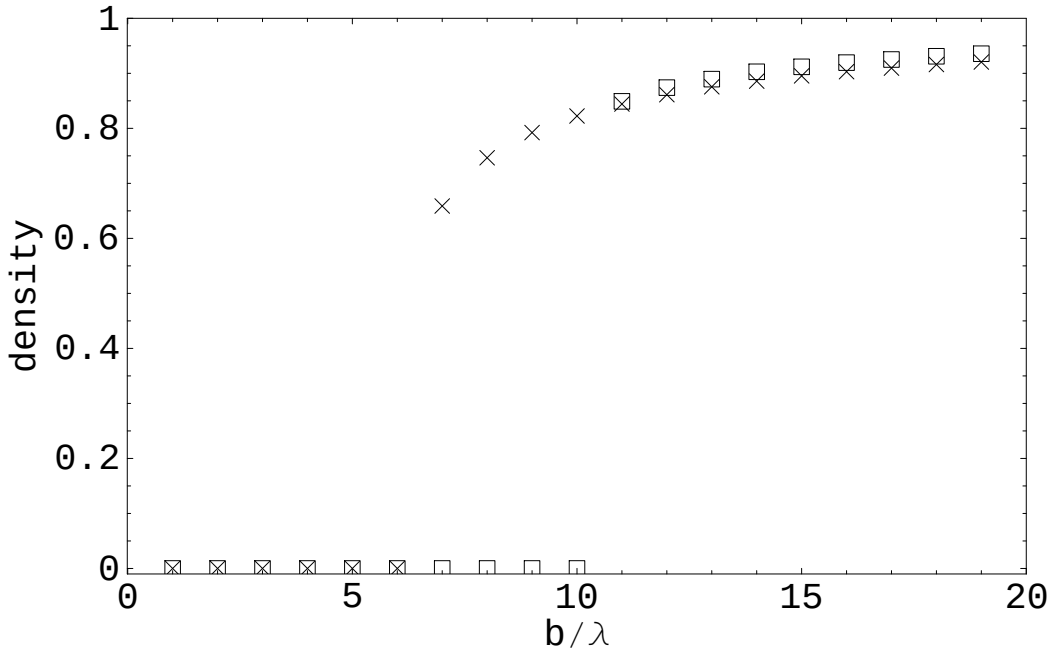

Figure 4.3: Hermaphrodite population density after 10^3 generations for lattice simulation of QCP (□) and MQCP (×). $L = 100$.

For the MQCP a transition from a stable active phase to stable absorbing phase occurs at $b_3/\lambda \approx 6$ (figure 4.3) . This is in contrast to the mean-field approximation, which predicts that the transition in the MQCP model should occur at a larger value of b/λ larger than in the QCP (see figure 4.1). These results demonstrate that the finite size effects specific to the QCP do have a significant impact on stability.

Investigations of the dynamics of the interface between active and absorbing states in the QCP [82, 83] showed that the active phase grows fastest (recedes slowest) for an interface orientation of 45° to the rows of the square lattice. This rate of growth (reduction) decreases (increases) as the angle of orientation is changed from 45°. For an interface orientation of 0° or 90° to the lattice rows, the active state cannot invade the absorbing state. This is because an empty site needs at least two diagonally adjacent nearest neighbours to become occupied. This results in the feature that if a population is contained inside a rectangle it can never give birth outside the rectangle [77] and for lattices of finite size, complete columns or rows of empty sites cannot become occupied. For an interface orientation of 0° or 90°, in the MQCP, the active state can invade the absorbing state. This is expected to be the reason for the contrast between simulation and mean-field behaviour in the QCP and MQCP.

Due to finite size effects, analysis of size dependent behaviour is required to accurately determine the stability regions [82, 83]. The exact values of these parameters are not calculated here but the stability of the two phases is clarified by plotting waiting time to extinction of the population as a function of lattice size L (figures 4.4 and 4.6). Each point in figures 4.4 and 4.6 is the mean waiting time to extinction from 100 simulation runs; each run was initialised with a fully occupied lattice and lattice sites were set to male with probability 0.5 for dioecious models. Figure 4.4 shows that in the stable active phase extinction time increases exponentially with L. The solid lines in figure 4.4 are least

squares fits for the data, their equations are given by;

$$\tau = \exp[2.98 + 0.471L], \quad \text{for QCP hermaphrodite,} \tag{4.4.1}$$

$$\tau = \exp[2.02 + 0.263L], \quad \text{for QCP dioecious,} \tag{4.4.2}$$

$$\tau = \exp[-192 + 1.00L], \quad \text{for MQCP hermaphrodite,} \tag{4.4.3}$$

$$\tau = \exp[0.802 + 0.450L], \quad \text{for MQCP dioecious,} \tag{4.4.4}$$

where $\tau = \lambda t$ is referred to as the time in generations (t is in Monte Carlo steps).

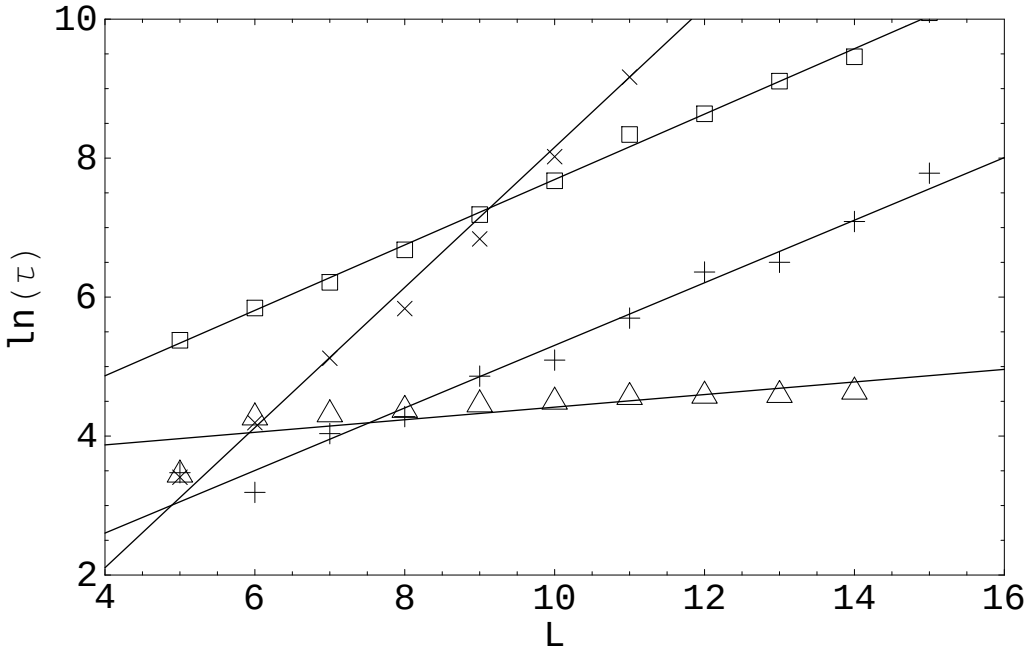

Figure 4.4: The natural logarithm of waiting time to extinction plotted against length of lattice side L, for: QCP hermaphrodite (□) with $b_1/\lambda = 11$, QCP dioecious (△) with $b_2/\lambda = 300$, MQCP hermaphrodite (×) with $b_3/\lambda = 7$, and MQCP dioecious (+) with $b_4/\lambda = 120$. The fitted lines are given by equations (4.4.1)–(4.4.4)

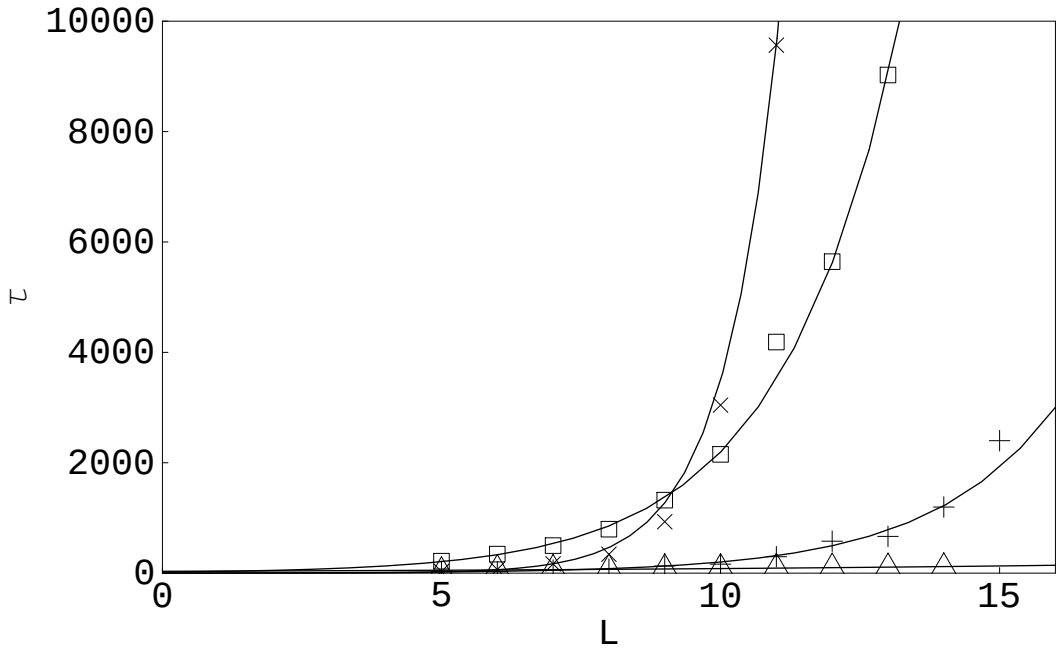

Figure 4.5: Waiting time to extinction plotted against length of lattice side L for the results shown in figure 4.4.

In the stable absorbing phase, figure 4.5 shows that the extinction time increases logarithmically with L. The solid lines in figure 4.4 are least squares fits for the data, their equations are given by;

$$\tau = \quad 11.2 + 18.4 \ln(L), \qquad \text{for QCP hermaphrodite,} \tag{4.4.5}$$

$$\tau = \quad -101 + 62.0 \ln(L), \qquad \text{for QCP dioecious,} \tag{4.4.6}$$

$$\tau = \quad -119 + 85.1 \ln(L), \qquad \text{for MQCP hermaphrodite,} \tag{4.4.7}$$

$$\tau = \quad -119 + 85.1 \ln(L), \qquad \text{for MQCP dioecious.} \tag{4.4.8}$$

Figure 4.8 plots the population density $(m + f)$ as a function of b/λ for the dioecious population. A discontinuous phase transition between the active and

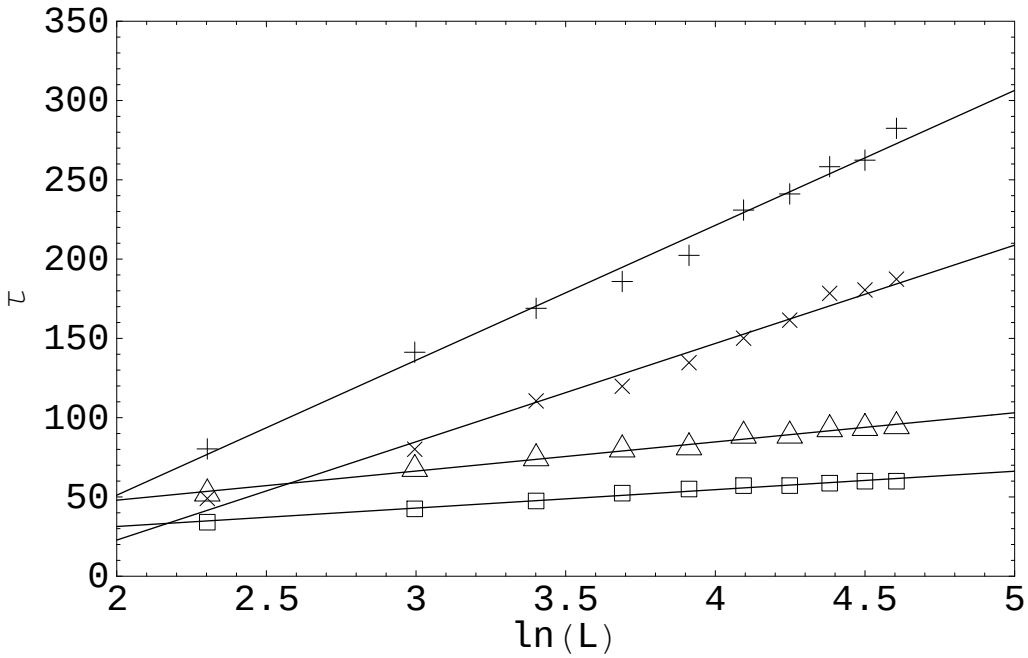

Figure 4.6: Waiting time to extinction plotted against the natural logarithm of length of lattice side L, for: QCP hermaphrodite ($\square$) with $b_1/\lambda = 9$, QCP dioecious ($\triangle$) with $b_2/\lambda = 100$, MQCP hermaphrodite ($\times$) with $b_3/\lambda = 6$, and MQCP dioecious ($+$) with $b_4/\lambda = 100$. The fitted lines are given by equations (4.4.5)–(4.4.8).

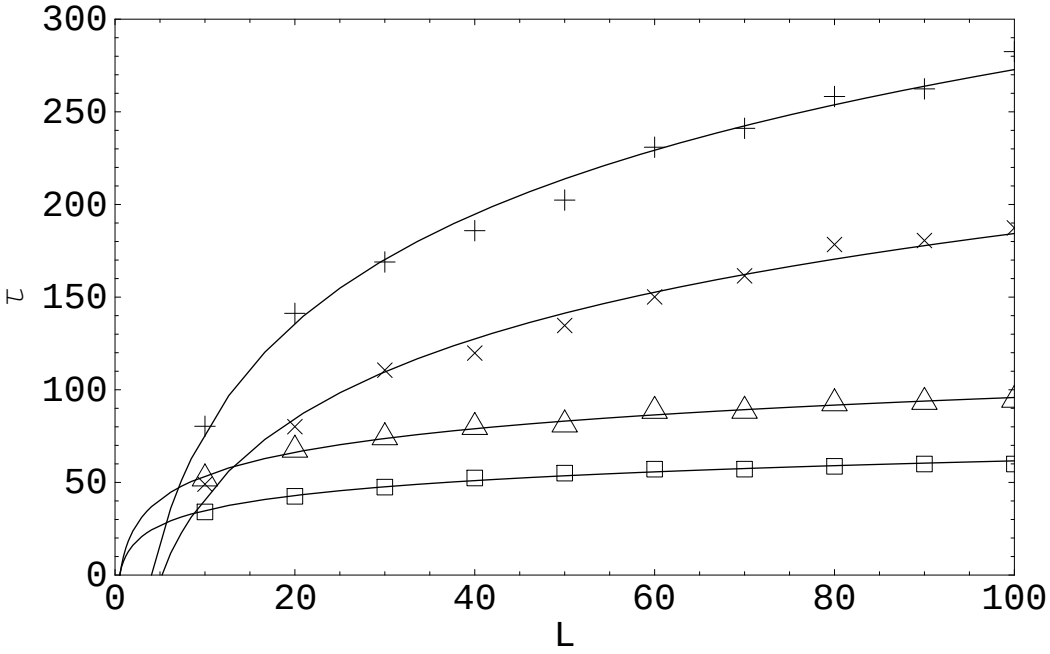

Figure 4.7: Waiting time to extinction plotted against length of lattice side L for results shown in figure 4.6.

absorbing states is observed at $b_2/\lambda \approx 300$ for the QCP and $b_4/\lambda \approx 100$ for the MQCP. Given more time, the two QCP points at densities close to 0.3 fall to zero. These slow relaxations close to the transition were also observed by Tainaka [81] and may be due to a metastable region, similar to the one observed for the QCP [82, 83]. Again, the stability of the two phases were clarified by plotting waiting time to extinction of the population as a function of lattice size L (figures 4.5 and 4.7). These results demonstrate that, as expected, finite size effects specific to the QCP do have a significant impact on the stability of dioecious populations on a lattice.

The transition from the active to absorbing phase in the QCP occurs at a value of b/λ 30 times larger in the dioecious population than the hermaph-

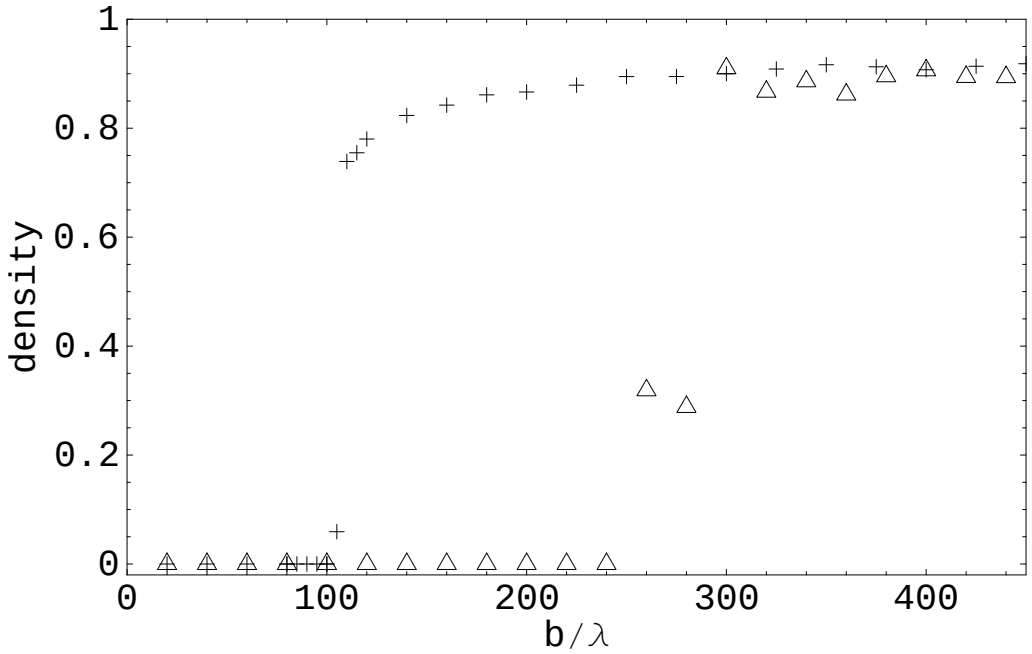

Figure 4.8: Sum of male and female densities, $m + f$, versus b/λ after 10^3 generations for QCP ($\triangle$) and MQCP ($+$). Each value of b/λ is initialised with a fully populated lattice where each lattice site was set to male with a probability 0.5. The densities plotted were averaged over the last 10^3 MCS of the simulation. $L = 100$.

rodite population (figures (4.3) and (4.8)). The transition from the active to absorbing phase in the MQCP occurs at a value of b/λ 15 times larger in the dioecious population than the hermaphrodite population (figures (4.3) and (4.8)). These results demonstrate more drastic differences between the hermaphrodite and dioecious mating systems than predicted by mean-field analysis (see figure 4.1). If birth rates were scaled such that hermaphrodites and females produce the same number of offspring ($b_4 = 2b_3$), all else being equal, this would correspond to a transition from absorbing to active state at a value of $b/\lambda \approx 7.5$ times larger in the dioecious MQCP model than the hermaphrodite MQCP.

Though the models predict different values for the advantage of single sex over dioecious populations on a lattice, both models suggest that a hermaphrodite population is stable over a large range of low birth rates for which a dioecious population is not sustainable. The relatively large birth rates required to sustain a dioecious population are likely to be due to local variation in the concentration of $(M - M)$ or $(F - F)$ pairs of cells, which hinder the birth process. As offspring are placed on nearest neighbour sites, areas with an optimum sex ratio (1/2) cannot compensate for areas with a poor sex ratio (close to 0 or 1). This can aid the propagation of the absorbing state. The observed advantage of hermaphroditism at low birth rates could contribute to the success of the hermaphrodite mating system in sedentary species. This provides additional support for the observations that hermaphroditism should be associated with sedentary species, such as plants and animals with poor mate search efficiency [76].

4.5 Conclusions and Future Investigations

By means of stochastic spatial simulations we have shown hermaphrodite populations can be sustainable at birth rates much smaller than the birth rates required for a sustainable dioecious population. This implies that a hermaphrodite population has a much greater reproductive advantage over a dioecious population than the the two-fold difference predicted by mean-field analysis. This result provides even greater theoretical support for the observations that hermaphroditism should be associated with sedentary species, such as plants and animals with poor mate search efficiency.

Extinction is an increasing concern worldwide. One of the central problems in conservation biology is to discover factors that influence the sustainability of populations. Knowledge of these factors could help in the introduction or reintroduction of populations in to habitats, and to eliminate pests. As explained earlier in this chapter, the Allee effect in a deterministic model predicts a critical population density above which the population grows to a stable equilibrium and below which the population becomes extinct. Similar effects have been observed in both macroscopic [84] and microscopic [85] stochastic models of the Allee effect in hermaphrodite populations. Knowledge of critical population numbers, required for a species to survive, may be of great use in conservation biology. Given the differences between dioecious and hermaphrodite populations observed in the simulations in this chapter, a valuable investigation would be to determine critical population numbers for dioecious populations, above

which the population can grow to fill an environment.

CHAPTER 5

Evolution of Gynodioecy

5.1 Introduction

Gynodioecy is a breeding system in plants where populations consist of hermaphrodite and female individuals. It is both a common and widespread polymorphism describing approximately 7% of all flowering plants [86], which includes species of ecological and economic interest. Gynodioecy is also an excellent system for studying the interplay of genetic architecture and ecology in evolution [87].

Gynodioecy occurs as a result of a genetic mutation which impairs pollen production in hermaphrodite plants. Genetic mutations can impair pollen production in several ways but still allow normal female reproduction [88]. The genetic basis for male sterility can significantly affect whether a mutation for male sterility can become established. Nuclear genes are inherited through both parents whereas cytoplasmic genes are only inherited from the mother. It has been

shown that females would need to be at least twice as fertile as hermaphrodites (produce twice as many offspring) for a nuclear male sterility gene to become established [89]. However, cytoplasmic male sterility can become established when the fertility of the female is only slightly larger than that of the hermaphrodite [89]. This is because a cytoplasmic gene is not inherited through male function and hence has nothing to lose if pollen production is stopped. In some species, male sterility is complicated futher by the evolution of restorer genes which suppress the deleterious effects of cytoplasmic male sterility [90].

Most previous models of inherited male sterility assume that female fitness is dependent on the number of pollinators in the environment and hermaphrodite fitness is independent of availability of pollinators because hermaphrodites could self-fertilise [89, 91]. However, if the case of a self-incompatible species is considered, cytoplasmic inherited male sterility is only stable if hermaphrodite and female fertility are exactly equal [92]. In this unlikely case it would be difficult for the cytoplasmic mutation to invade from small frequencies as it is neutral in terms of selection. For the case of cytoplasmic male sterility in out-crossing hermaphrodites, it was shown that if female fertility is larger than hermaphrodite fertility, females will spread until scarcity of pollen causes the population to become extinct [93].

A spatial model of cytoplasmic male sterility in self-incompatible hermaphrodites [93], showed behaviour vastly different from the predictions of non-spatial models. Where non-spatial models predicted that invasion of females would lead to extinction of the population (female fertility $>$ hermaphrodite

fertility), the spatial model [93] instead displayed stable nodes, foci, limit cycles or extinction depending on the relative fertility of females to hermaphrodites. This demonstrated that cytoplasmic male sterility can evolve in self-incompatible hermaphrodite populations.

In this chapter, the evolution of male sterility due to a dominant allele in a nuclear gene is investigated by use of stochastic spatial simulation and mean-field approximation. The conditions necessary for male sterility to evolve are calculated along with equilibrium frequency of females in the population. A knowledge of the equilibrium frequency of females may be of use when comparing the results of breeding experiments with observations of female frequency in the wild.

In section 5.2 the Modified Quadratic Contact Process (MQCP), which was introduced in chapter 4, is extended to model a population of females and self-incompatible hermaphrodites. Mean-field analysis (section 5.3) and stochastic spatial simulation (section 5.4) are used to investigate the conditions necessary for nuclear male sterility to evolve and the equilibrium frequency of females in the population. The MQCP demonstrates behaviour in agreement with previous spatial simulations [93] for the case of cytoplasmic male sterility.

5.2 Model

The population resides on a two-dimensional square lattice of side length L, with periodic boundary conditions. Each lattice site can be occupied by either

a self-incompatible hermaphrodite (H), a female (F) or be empty ($\oslash$). An occupied site becomes vacant at a rate λ, the death rate. The death rate is considered to be equal for hermaphrodites and females for the purposes of this model.

A hermaphrodite produces an offspring at a rate equal to $j\kappa_1/4$, where j is the number of nearest neighbour sites occupied by hermaphrodites and κ_1 is the birth rate. A nearest neighbour site is then chosen randomly. If the chosen site is empty the offspring is placed on the site. If the site is occupied the offspring is deleted. Similarly, a female produces a hermaphrodite offspring at a rate, $j\kappa_2/4$, and a female offspring at a rate, $j\kappa_3/4$. Thus, a female produces offspring at a total rate, $j(\kappa_2 + \kappa_3)/4$.

Genetics can be explicitly defined in this model for the case of a dominant allele in a nuclear gene that causes male sterility, or a cytoplasmic gene that causes male sterility. Consider a dominant nuclear allele for male sterility, B_1. Thus, $B_1B_2 =$ female, and, $B_2B_2 =$ hermaphrodite. Since females produce no pollen, no homozygous B_1B_1 individuals are formed and there are only two genotypes in the population [89]. $\kappa_2 \neq \kappa_3$, represents the case of differential mortality between male and female offspring due to their own sex genotypes [94].

The case of cytoplasmic male sterility is modelled by setting $\kappa_2 = 0$. Hence, females always produce females and the hermaphrodite population is not increased through mating with females.

5.3 Mean-field Analysis

The mean-field kinetics of the hermaphrodite and female populations are described by,

$$\frac{dh}{dt} = h\left[-\lambda + \frac{3\left(h\kappa_1 + f\kappa_2\right)\left(1-h-f\right)}{4}\right] \tag{5.3.1}$$

$$\frac{df}{dt} = f\left[-\lambda + \frac{3h\kappa_3\left(1-h-f\right)}{4}\right] \tag{5.3.2}$$

where h and f are the densities of hermaphrodites and females respectively. By scaling time ($\tau = \lambda t$), the system can be simplified by introducing the parameters; $K_1 = 3\kappa_1/4\lambda$, $K_2 = 3\kappa_2/4\lambda$ and $K_3 = 3\kappa_3/4\lambda$.

In the following mean-field analysis, the case of nuclear male sterility ($K_1 > 0$, $K_2 > 0$ and $K_3 > 0$) will be considered first and the case of cytoplasmic male sterility ($K_1 > 0$, $K_2 = 0$ and $K_3 > 0$) will be considered second.

5.3.1 Nuclear male sterility.

Equilibria for equations (5.3.1) and (5.3.2) were found by setting the time derivative equal to zero, then solving the resulting two equations simultaneously. The nature of these equilibria was characterised by linear stability analysis of the system of equations (5.3.1) and (5.3.2). As $h \geq 0$, $f \geq 0$ and $h + f \leq 1$, the region of interest on the (h,f)-plane is the triangle with vertices $(h = 0, f = 0)$, $(h = 1, f = 0)$ and $(h = 0, f = 1)$. The trivial equilibrium $(h = 0, f = 0)$ is stable provided $\lambda > 0$. For $(K_1 > 0, K_2 > 0, K_3 > 0)$, equations (5.3.1) and (5.3.2) have four equilibria besides the trivial one. Two equilibria are located on the

$(f = 0)$-boundary with,

$$h_2 = \frac{1}{2}\left(1 - \sqrt{\frac{K_1 - 4}{K_1}}\right), \tag{5.3.3}$$

$$h_3 = \frac{1}{2}\left(1 + \sqrt{\frac{K_1 - 4}{K_1}}\right). \tag{5.3.4}$$

The remaining two equilibria are,

$$h_4 = \frac{K_2K_3 - \sqrt{A}}{2K_3\left(K_2 + K_3 - K_1\right)}, \tag{5.3.5}$$

$$f_4 = \frac{\left(K_3 - K_1\right)\left(K_2K_3 - \sqrt{A}\right)}{2K_2K_3\left(K_2 + K_3 - K_1\right)}, \tag{5.3.6}$$

$$h_5 = \frac{K_2K_3 + \sqrt{A}}{2K_3\left(K_2 + K_3 - K_1\right)}, \tag{5.3.7}$$

$$f_5 = \frac{\left(K_3 - K_1\right)\left(K_2K_3 + \sqrt{A}\right)}{2K_2K_3\left(K_2 + K_3 - K_1\right)}, \tag{5.3.8}$$

where $A = K_2K_3\left[4\left(K_1 - K_2 - K_3\right) + K_2K_3\right]$. Eigenvalues and eigenvectors from the linear stability analysis of these equilibria can be found in appendix A.1.

Equilibria $(h_2, 0)$ and $(h_3, 0)$ are real and positive only if $K_1 > 4$. The eigenvalues from the linear stability analysis of these equilibria are only dependent on K_1 and K_3. If $K_1 > K_3$, equilibria $(h_2, 0)$ and $(h_3, 0)$ are a saddle point and attractor respectively. Thus, a small number of mutant females cannot invade a hermaphrodite population. This marks a regime where hermaphroditism is an ESS. Later it will be shown that when $K_1 > K_3$, only equilibria $(0, 0)$, $(h_2, 0)$ and $(h_3, 0)$ exist in the region of interest. Typical dynamics for the regime, where $K_1 > 4$ and $K_1 > K_3$, are shown in figure 5.1. The unstable manifold of the saddle point in figure 5.1 lies along the $(f = 0)$-boundary. Thus, a population of just hermaphrodites evolves to the trivial equilibrium if the initial density of

the population is below the saddle point and evolves to the stable node if the initial density of the population is above the saddle point.

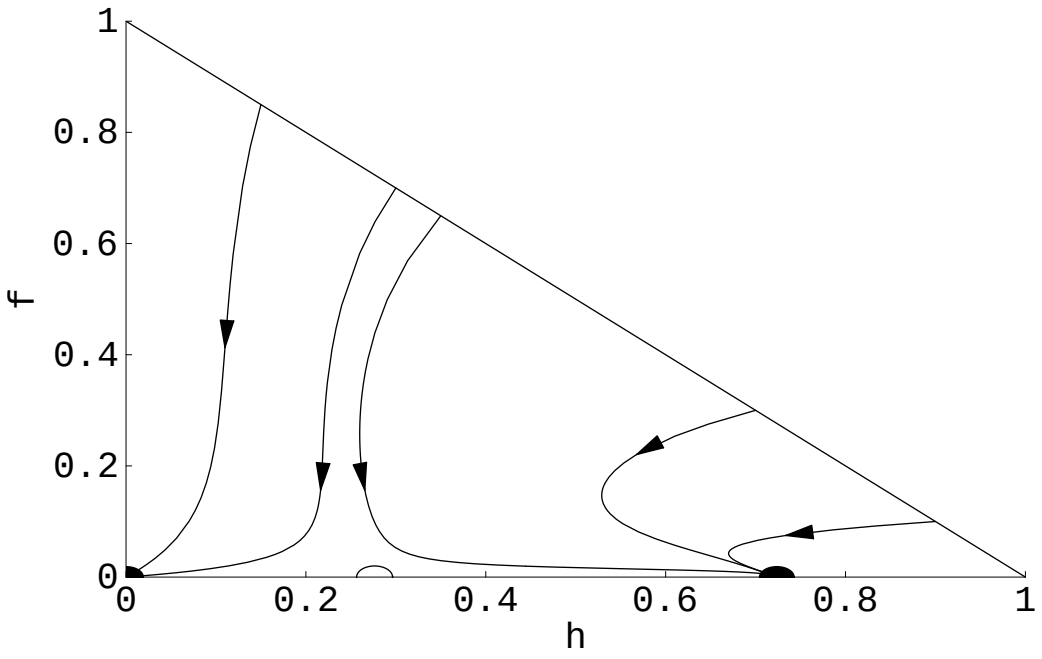

Figure 5.1: Typical mean-field dynamics for the case where hermaphroditism is the ESS. Filled circles mark stable nodes, the empty circle marks a saddle point. The arrows indicate the direction of evolution. Plot shown for $K_1 = 5$, $K_2 = 3$ and $K_3 = 3$.

If $K_3 > K_1$, equilibria $(h_2, 0)$ and $(h_3, 0)$ are an unstable node and saddle point respectively. The unstable manifold of the saddle point at $(h_3, 0)$ points in to the interior, $(h > 0, f > 0)$. In the absence of females the dynamics of the hermaphrodite population is the same as for the case, $K_1 > K_3$. However, a small number of mutant females can now invade the hermaphrodite population. Thus, Hermaphroditism is no longer an ESS.

By inspecting equations (5.3.5)-(5.3.8) it can be seen that equilibria (h_4, f_4)

and (h_5, f_5) are real only if $A > 0$. Using this condition, it can be shown that equilibria (h_4, f_4) and (h_5, f_5) are positive and real if,

$$\begin{aligned} K_3 &> 4, \\ K_3 &> K_1, \\ \text{and} \quad K_2 &> S, \end{aligned} \tag{5.3.9}$$

where,

$$S = \frac{4K_3 - 4K_1}{K_3 - 4}. \tag{5.3.10}$$

When they exist in the region of interest, equilibria (h_4, f_4) and (h_5, f_5) are a saddle point and stable node respectively. The condition, in equation (5.3.9), that $K_3 > K_1$, means that the boundary equilibrium $(h_2, 0)$ and $(h_3, 0)$ are an unstable node and a saddle point respectively. Thus, when conditions in equation (5.3.9) are satisfied, a small number of females will always invade a hermaphrodite population, the population can then evolve to the stable node (h_5, f_5). Under these conditions, a coexisting population of hermaphrodites and females is stable. Typical dynamics for this regime are shown in figure (5.2).

The conditions in equations (5.3.9) also reveal that a coexisting population of females and hermaphrodites can be stable even when a population consisting solely of hermaphrodites is not stable (when $K_1 < 4$). Typical dynamics for this regime is shown in figure 5.3.

Whilst obeying equations (5.3.9), reducing K_3 (or increasing K_1) brings equilibria (h_4, f_4) and (h_5, f_5) closer to the $(f = 0)$-boundary. Equilibria (h_4, f_4) and

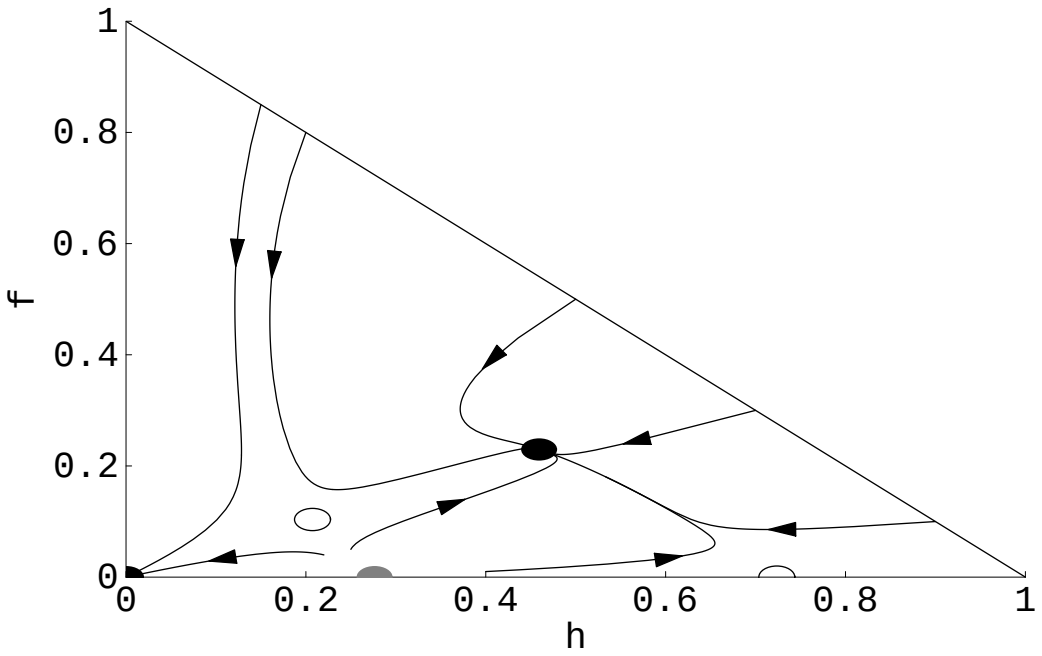

Figure 5.2: Typical mean-field dynamics for the case where a coexisting population of hermaphrodites and females is evolutionary stable. Filled circles mark stable nodes, empty circles mark saddle points and the grey filled circle marks an unstable node. The arrows indicate the direction of evolution. Plot shown for $K_1 = 5$, $K_2 = 4$ and $K_3 = 7$.

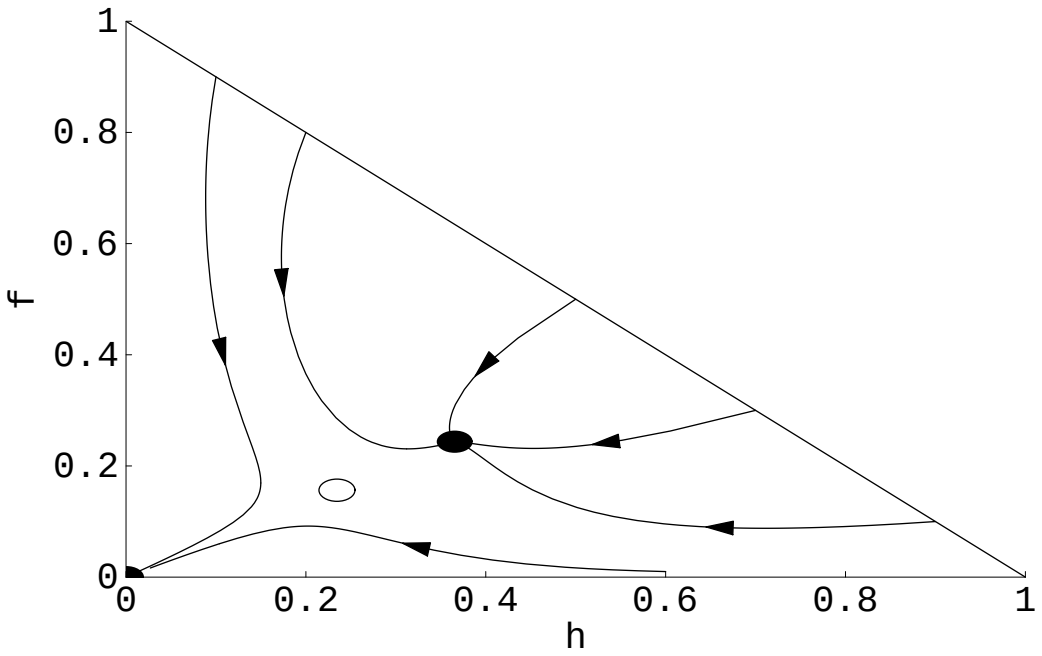

Figure 5.3: Typical mean-field dynamics for a coexisting population of hermaphrodites and females. $K_1 < 4$, so there are no $(f = 0)$-boundary equilibrium. Filled circles mark stable nodes and the empty circle marks a saddle point. The arrows indicate the direction of evolution. Plot shown for $K_1 = 3$, $K_2 = 6$ and $K_3 = 7$.

(h_5, f_5) collide with the boundary equilibrium, $(h_2, 0)$ and $(h_3, 0)$ respectively, at $K_3 = K_1$, here a transcritical bifurcation occurs. As discussed above, when $K_1 > K_3$, the $(f = 0)$ boundary equilibria $(h_2, 0)$ and $(h_3, 0)$ are a saddle point and attractor respectively. Thus hermaphroditism is the ESS.

Decreasing K_2, whilst obeying the conditions in equation 5.3.9, brings equilibria (h_4, f_4) and (h_5, f_5) closer together. At $K_2 = S$, equilibria (h_4, f_4) and (h_5, f_5) collide and annihilate. This is a saddle-node bifurcation point. If $K_3 > K_1$ and $K_2 < S$; the $(f = 0)$-boundary equilibria, $(h_2, 0)$ and $(h_3, 0)$, are a node and saddle point respectively and no equilibrium for coexistence exists. Under these conditions females could invade the hermaphrodite population. As the only stable equilibrium is the trivial equilibrium the population will then converge on the trivial equilibrium, resulting in extinction. Typical dynamics for this regime are shown in figure 5.4.

All possible evolutionary outcomes for the case $K_1 > 0$, $K_2 > 0$ and $K_3 > 0$ are summarised in table (5.1). At equilibrium the frequency of females in the population is given by,

$$\frac{f_5}{f_5 + h_5} = \frac{K_3 - K_1}{K_3 + K_2 - K_1}, \tag{5.3.11}$$

which is consistent with previous results for nuclear male sterility from population genetics [89]. Note that equation (5.3.11) is only valid if the (h_5, f_5) is real and positive, therefore if the conditions in equation 5.3.9 are satisfied.

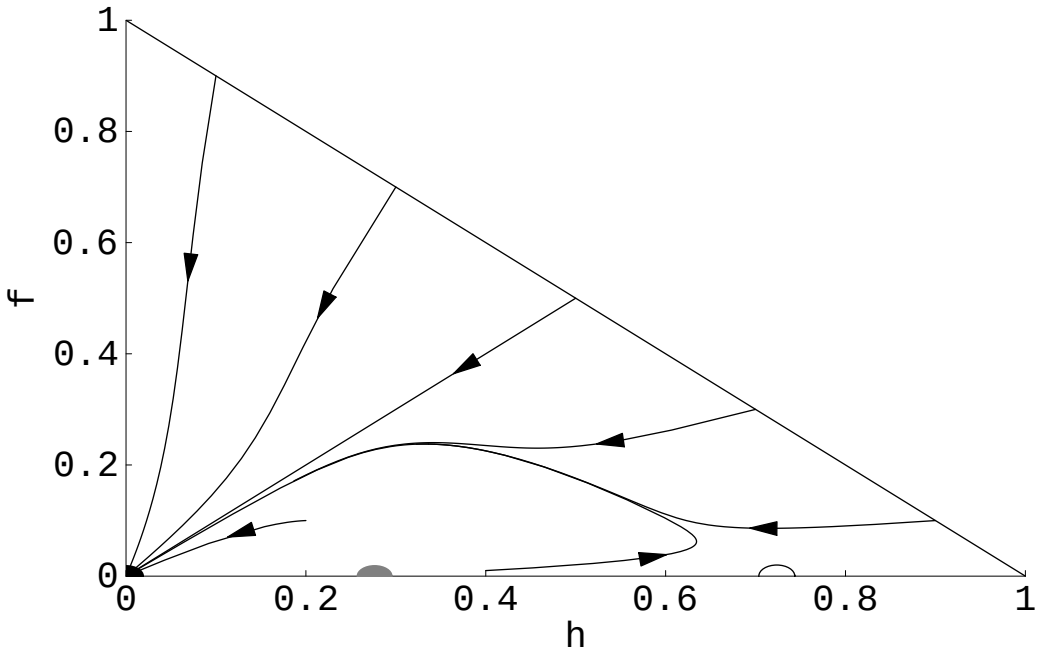

Figure 5.4: Typical mean-field dynamics for the case where invasion of females leads to extinction. Filled circles mark stable nodes, the empty circle marks a saddle points and the grey filled circle marks an unstable node. The arrows indicate the direction of evolution. Plot shown for $K_1 = 5$, $K_2 = 2$ and $K_3 = 7$.

	$K_1 > 4$	$K_1 < 4$
$K_1 > K_3$	H is ESS	extinction (only trivial equilibrium)
$K_3 > K_1$ & $S < K_2$	female invasion leads to extinction	extinction (only trivial equilibrium)
$K_3 > K_1$ & $K_2 > S$ & $K_3 > 4$	coexistence	coexistence

Table 5.1: Evolutionary outcomes in mean-field analysis, for nuclear male sterility ($K_1 > 0, K_2 > 0, K_3 > 0$).

5.3.2 Cytoplasmic male sterility

For the case of cytoplasmic male sterility, the behaviour of equilibria $(h_2, 0)$ and $(h_3, 0)$ is same as in the previous section; for $K_1 > K_3$ equilibria $(h_2, 0)$ and $(h_3, 0)$ are a a saddle point and stable node respectively, for $K_3 < K_1$ equilibria $(h_2, 0)$ and $(h_3, 0)$) are an unstable node and saddle point respectively.

If $K_2 = 0$ and $K_1 > K_3$, hermaphroditism is an ESS and similar dynamics to those shown in figure 5.1 are observed. For $K_2 = 0$ and $K_3 > K_1$, females can invade a hermaphrodite population but the population then converges on the trivial equilibria and becomes extinct. The dynamics observed for this case are similar to those shown in figure 5.4.

For the special case $K_2 = 0$ and $K_3 = K_1$, there is a curve of equilibrium points given by,

$$f = \frac{K_1 h - K_1 h^2 - 1}{K_1 h}. \tag{5.3.12}$$

Eigenvalues and eigenvectors from the linear stability analysis of this equilibrium curve are given in appendix A.2. The first eigenvalue for points on this equilibrium curve is zero with corresponding eigenvector along the curve. The second eigenvalue is negative for $h > 2/K_1$ and positive for $h < 2/K_1$. Typical dynamics for this regime is shown in figure 5.5. The behaviour observed here for the case $K_2 = 0$ is in agreement with previous results from similar evolutionary models [92, 93].

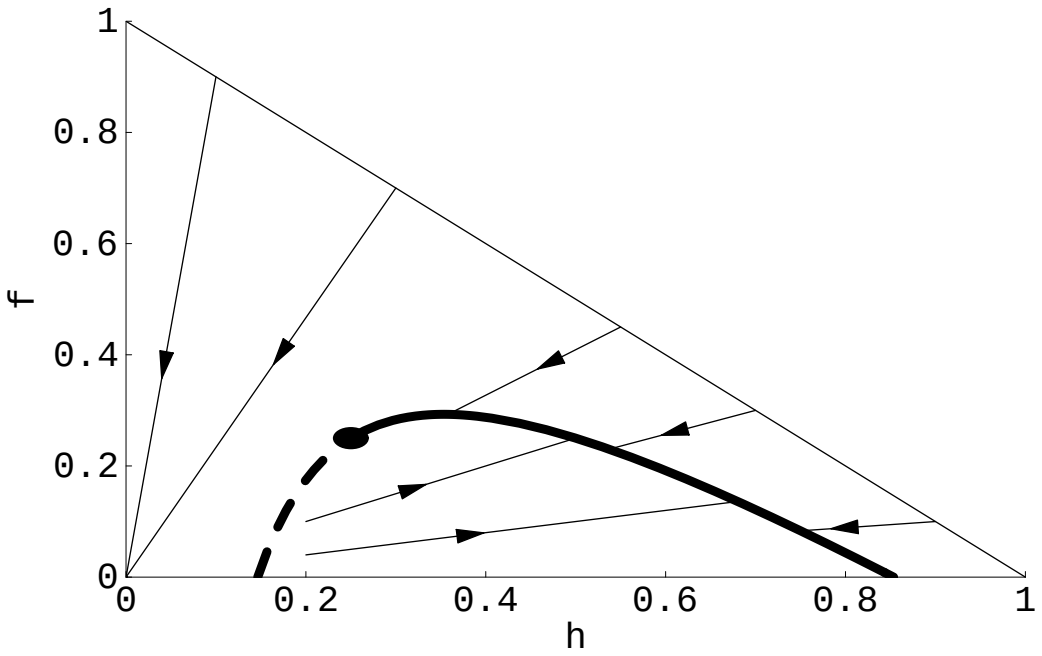

Figure 5.5: Typical mean-field dynamics for the case where of a curve of equilibrium points. Plot shown for $K_1 = K_3 = 8$, $K_2 = 0$. The solid section of the curve is stable, the dashed section is unstable. The filled circle indicates the point at which the curve becomes unstable. The arrows indicate the direction of evolution.

5.4 Results of lattice simulation

All simulations were run on lattices of side length L for 100 generations, where the time in generations is given by $\tau = \lambda t$, and t is in Monte Carlo steps.

The simulation results for the case of cytoplasmic male sterility ($K_2 = 0$) are in agreement with previous spatial simulations [93]. Simulations (for $K_2 = 0$) display coexistence of females and hermaphrodites for values of K_3 moderately larger than K_1 (figure 5.6). Figure 5.7 shows how behaviour is increasingly cyclic with increased female reproductive advantage (increased K_3/K_1). This contrasts with mean-field kinetics, which predict extinction of the population following the invasion of females (figure 5.4). Large vales of K_3 result in extinction (not shown) showing similar behaviour to mean-field predictions (figure 5.4).

Sample paths from the lattice simulation for the case of nuclear male sterility are shown in figures 5.8 and 5.9. In figure 5.8, hermaphroditism is the ESS. It can be seen from the plot, that the hermaphrodite population is robust against invasion by large numbers of females. This is in agreement with mean-field kinetics. In figure 5.9, coexistence of females and hermaphrodites is evolutionary stable. The paths shown in figure 5.9 converge on an equilibrium at approximately $(0.77, 0.12)$. This is difficult to see from figure 5.9 due to slow dynamics close to the equilibrium.

Breaking the condition $K_2 > S$ (equation (5.3.9)) with $K_3 > K_1$ does not

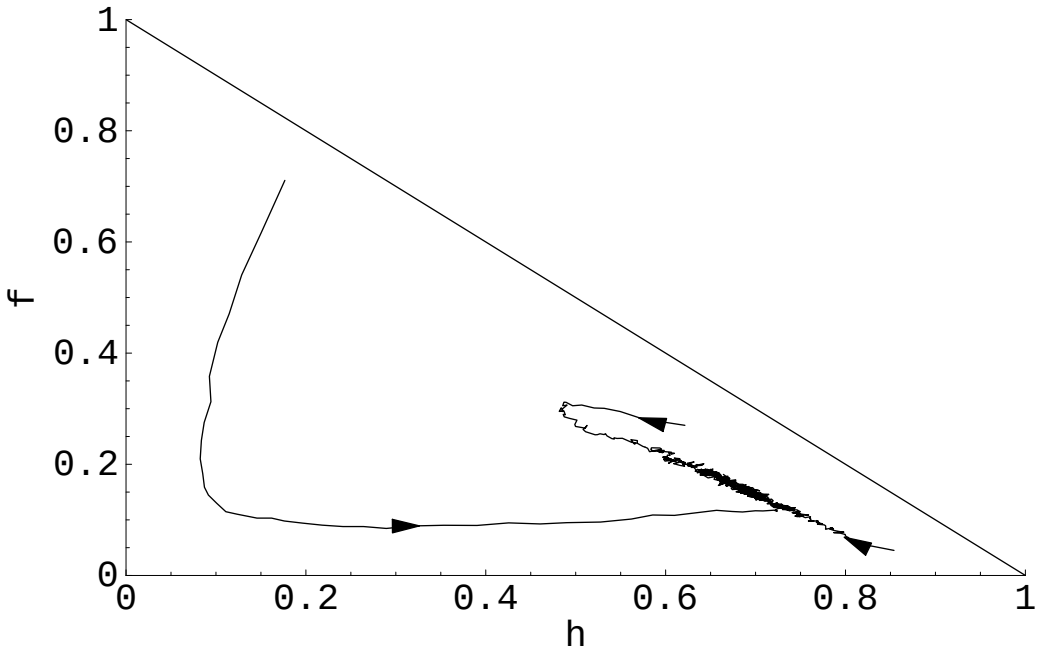

Figure 5.6: Lattice simulation for cytoplasmic male sterility; coexistence of females and hermaphrodites. The arrows indicate the direction of evolution. Plot shown for $K_1 = 10$, $K_2 = 0$ and $K_3 = 20$.

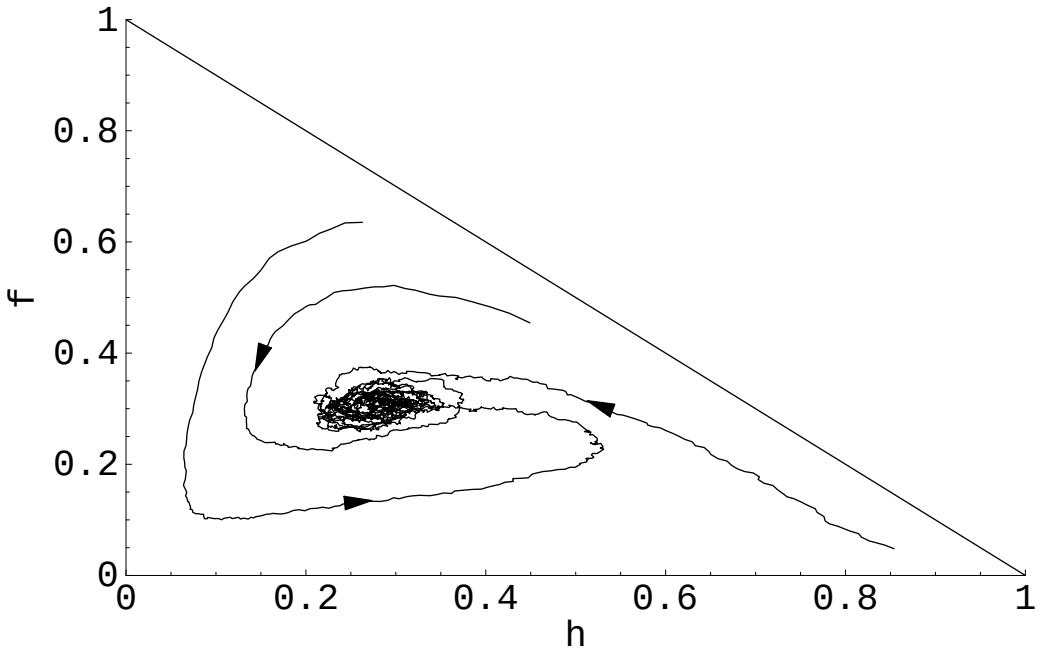

Figure 5.7: Lattice simulation for cytoplasmic male sterility; coexistence of females and hermaphrodites. The arrows indicate the direction of evolution. Plot shown for $K_1 = 10$, $K_2 = 0$ and $K_3 = 40$.

result in extinction following female invasion, as predicted by mean-field analysis. Instead simulations display coexistence with increasingly cyclic behaviour as K_2 is decreased and/or K_3 increased. This result is not surprising given the observations for $K_2 = 0$ shown earlier (figures 5.6 and 5.7).

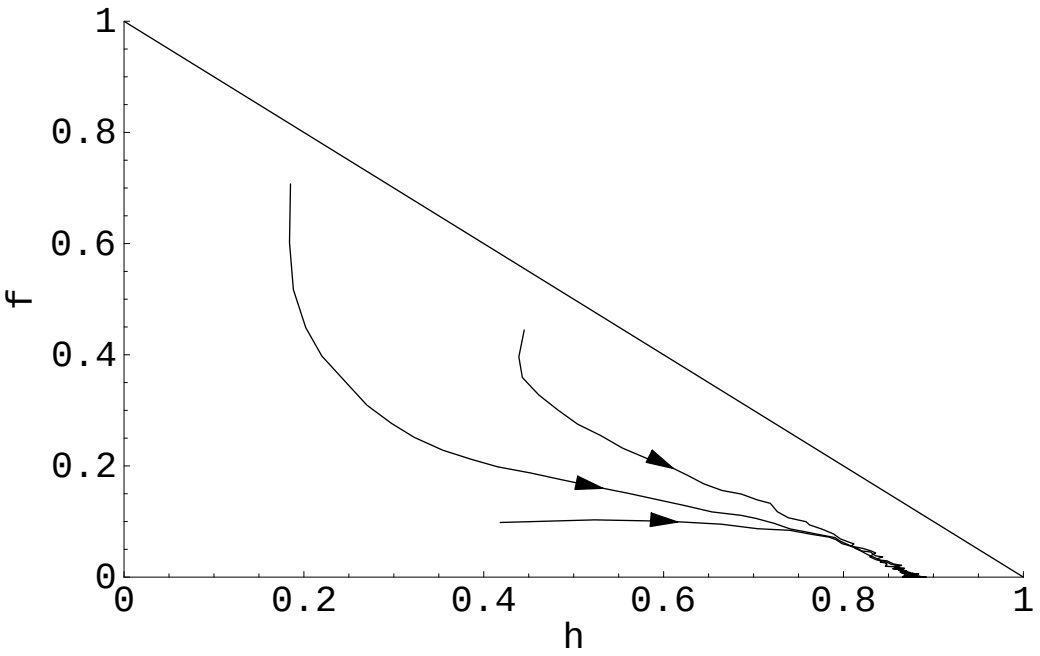

Figure 5.8: Lattice simulation; hermaphroditism is an ESS. The arrows indicate the direction of evolution. Simulations were run for 100 generations on a lattice of side length $L = 100$ with $K_1 = 10$, $K_2 = 8$ and $K_3 = 8$.

The frequency of females in natural gynodioecious populations is often used as an indicator of the genetic mechanism responsible for male sterility in a particular species [87]. For the case of nuclear male sterility where $K_2 > S$, spatial simulations arrive at equilibria which are fairly static in (h, f)-space. Thus equilibrium frequencies of females in the population are easily calculated. Figure

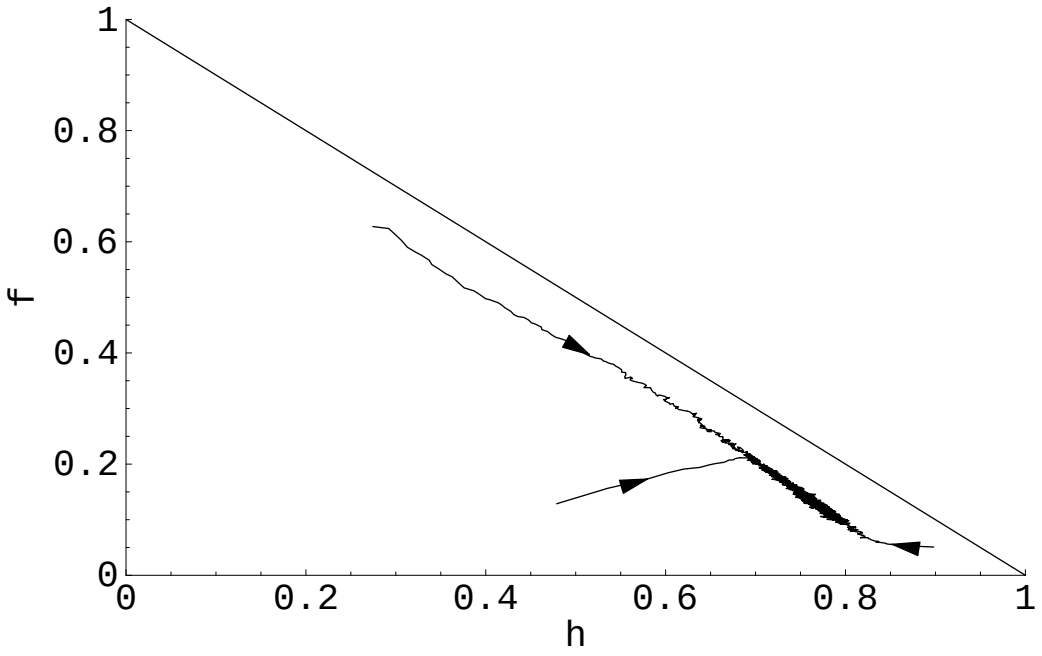

Figure 5.9: Lattice simulation; coexistence of females and hermaphrodites. The arrows indicate the direction of evolution. Simulations were run for 100 generations on a lattice of side length $L = 100$ with $K_1 = 10$, $K_2 = 40$ and $K_3 = 40$.

5.10 plots the equilibrium female frequencies for spatial simulation and mean-field analysis as a function of K_3/K_1, with $K_2 = K_3$. For each set of results K_1 was fixed while K_2 and K_3 were incremented. By testing several values of K_1, the plots show that the relative magnitudes of K_1, K_2 and K_3 are dominant in determining the behaviour of the system and not their absolute values. Though birth rates do need to be of sufficient magnitude to avoid extinction, as discussed in the previous chapter.

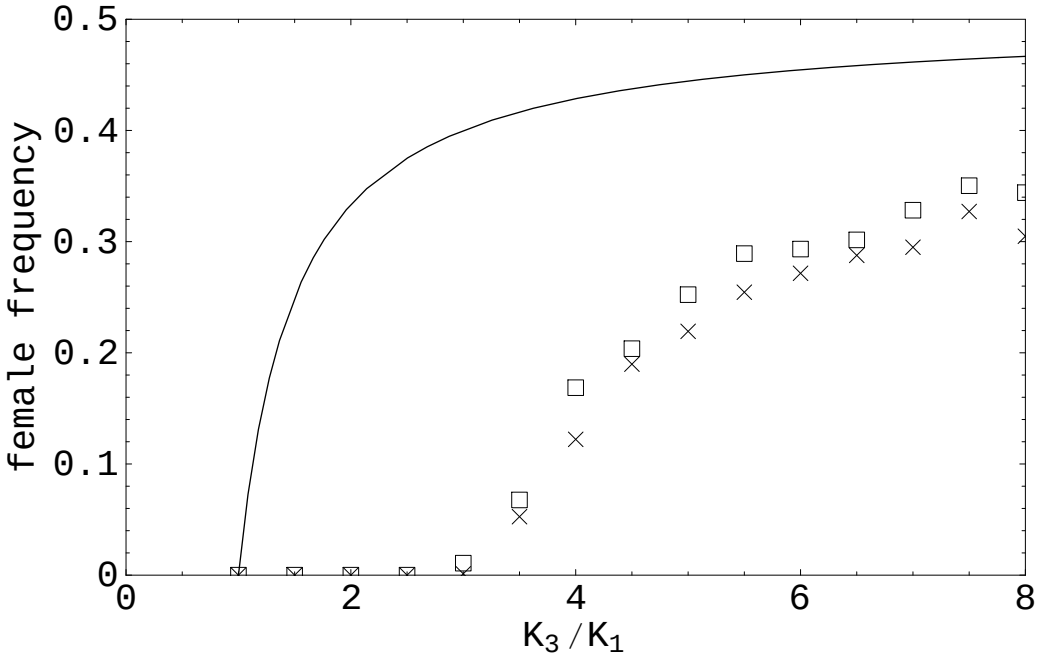

Figure 5.10: Comparison of equilibrium sex-ratio for mean-field (line) and lattice simulation (×). Simulations shown for $K_2 = K_3$, and $K_1 = 10$ (□) and $K_1 = 20$ (×). Points shown were averaged over the last 10 generations of the simulation.

Mean-field analysis predicted that nuclear male sterility could evolve if $K_3 > K_1$. Figure 5.10 shows that the condition for nuclear male sterility to evolve in

a spatial simulation with ($K_2 = K_3$) is approximately $K_3 > 3K_1$. This infers that nuclear male sterility is less likely to evolve in species with local pollination and seed setting, as is the case in the simulation.

Figure 5.10 also shows that female frequency is lower in the spatial simulation than predicted by mean-field analysis. Thus, it may be expected that gynodioecious plant species with local pollination and seed setting should have lower female frequencies in the wild compared to species with long range pollen interaction. This difference between mean-field and simulation is probably due to regions of high female concentration in the spatial simulation dying off because of pollen shortage.

5.5 Conclusions and future investigations

The population dynamics for a stochastic spatial simulation and its mean-field approximation have been presented for a gynodioecious population where male sterility is conferred by a dominant nuclear allele. It was demonstrated that a female needs a much greater fertility advantage to become established in the stochastic spatial simulation when compared with the mean-field approximation. This result suggests that gynodioecy is less likely to evolve in plants with local pollination and seed setting. This also, has implications for the evolution of dioecy, as gynodioecy is thought to be a route to dioecy [95].

The equilibrium frequency of females in the population was found to be smaller in the stochastic spatial simulation than in the mean-field approxima-

tion. This suggests that a lower frequency of females should be expected for gynodioecious populations with local pollination and seed setting.

This method of simulation could be applied to related problems in the evolution of sexual function, and could also be tailored to accommodate the specific details of the species in question. For example the case presented above was for self-incompatible hermaphrodites. In many species some self-fertilisation is observed in addition to out-crossing [96]. This could be an interesting addition to the model described in this chapter.

As pointed out in the introduction, male sterility has also been observed to be controlled by more complex genetic interactions than studied here. For example male sterility due to recessive genes [89], the evolution of restorer genes which counter male sterility [90]. Spatial simulations similar to the one presented here could easily be applied to these systems.

CHAPTER 6

Conclusions

Conclusions from the four sections of this thesis are summarised here.

Firstly, in chapter 2, it was shown that certain anomalies arise in the Penna bit-string model of ageing that lead to unusual demographic distributions and the so-called "Eve effect". It was shown that these anomalies were associated with diffusing subpopulation numbers hitting an absorbing barrier at zero, which in turn reduced the genetic variability of the population. This process is similar in nature to the well known first-passage problem. The analytical solution derived in this chapter to describe the unusual demographic distributions which arose was in excellent agreement with simulation results.

Secondly, in chapter 3, evolutionary game theory was applied to the evolution of harmful mating tactics in hermaphrodites. The analysis showed that harmful mating strategies are likely to be associated with species in which sperm precedence strongly favours the first mate. Though this criterion becomes less important as harmful tactics become more efficient. It was also

shown that a strongly female biased resource allocation strategy should be associated with harmful mating tactics, and that very high levels of harm can be adaptive. These inferences should prove useful in the interpretation of empirical observations involving harmful mating in hermaphrodites.

Thirdly, in chapter 4, two different stochastic spatial simulations were used to investigate the sustainability of hermaphrodite and dioecious populations. It was shown that when interactions are local (spatial simulation), hermaphrodites have a much greater advantage over dioecious populations than predicted by mean-field analysis. This may contribute to the success of hermaphroditism as a mating strategy in sedentary species. It was also shown that finite size effects associated with one of the spatial simulations (the QCP) can greatly affect the stability of the active state (finite population). These results may be of interest for other applications of the QCP in chemical, ecological and sociological systems.

Finally, in chapter 5, the evolution of gynodioecy in self-incompatible hermaphrodites was investigated for the case of male sterility conferred by a dominant nuclear allele. Population dynamics were presented for stochastic spatial simulation and mean-field approximation. It was shown that, when interactions are local (spatial simulation), male sterility conferred by a dominant nuclear allele requires a greater female fertility to evolve than predicted by mean-field approximations. This suggests that gynodioecy is less likely to evolve in plants with local pollination and seed setting. It was also observed that the spatial simulations resulted in a lower female frequency than predicted by mean-

field approximation. This may be useful in the interpretation of empirical observations.

APPENDIX A

Stability Analysis of gynodioecious population.

The stability of each equilibrium point was characterised by performing a Taylor expansion of equations (5.3.1) and (5.3.2) about the equilibrium, then calculating the eigenvalues of the resulting linearised system of equations. The eigenvalues and corresponding eigenvectors for this analysis are presented below.

A.1 Nuclear male sterility

The equilibrium points for nuclear male sterility are given in equations (5.3.3) – (5.3.8). The eigenvalues for the trivial equilibrium $(0, 0)$ are,

$$\nu_1^1 = -1, \tag{A.1.1}$$

$$\nu_1^2 = -1, \tag{A.1.2}$$

with corresponding eigenvectors,

$$\mathbf{z_1^1} = (0,1), \tag{A.1.3}$$

$$\mathbf{z_1^2} = (1,0). \tag{A.1.4}$$

The eigenvalues for $(h_2, 0)$ are,

$$\nu_2^1 = \frac{4 - K_1 + \sqrt{K_1 (K_1 - 4)}}{2}, \tag{A.1.5}$$

$$\nu_2^2 = \frac{K_3}{K_1} - 1, \tag{A.1.6}$$

with corresponding eigenvectors,

$$\mathbf{z_2^1} = (1,0), \tag{A.1.7}$$

$$\mathbf{z_2^2} = \left(\frac{K_1 \left(2 - K_1 + \sqrt{K_1 (K_1 - 4)} \right) + 2K_2}{K_1 \left(K_1 - 6 - \sqrt{K_1 (K_1 - 4)} \right) + 2K_3}, 1 \right). \tag{A.1.8}$$

The eigenvalues for $(h_3, 0)$ are,

$$\nu_3^1 = \frac{4 - K_1 - \sqrt{K_1 (K_1 - 4)}}{2}, \tag{A.1.9}$$

$$\nu_3^2 = \frac{K_3}{K_1} - 1, \tag{A.1.10}$$

with corresponding eigenvectors,

$$\mathbf{z_3^1} = (1,0) \tag{A.1.11}$$

$$\mathbf{z_3^2} = \left(\frac{K_1 \left(2 - K_1 - \sqrt{K_1 (K_1 - 4)} \right) + 2K_2}{K_1 \left(K_1 - 6 + \sqrt{K_1 (K_1 - 4)} \right) + 2K_3}, 1 \right). \tag{A.1.12}$$

The eigenvalues of $(h_4, 0)$ are,

$$\nu_4^1 = \frac{K_1}{K_3} - 1, \tag{A.1.13}$$

$$\nu_4^2 = \frac{2}{1 + K_2 K_3 A^{-1/2}}, \tag{A.1.14}$$

where $A = K_2K_3\left[4\left(K_1 - K_2 - K_3\right) + K_2K_3\right]$. The corresponding eigenvectors are,

$$\mathbf{z_4^1} = \left(\frac{-K_2\left(2K_1 + K_2\left(K_3 - 2\right) - 4K_3 + A^{1/2}\right)}{K_3\left(2K_1 + K_2\left(K_3 - 4\right) - 2K_3 + A^{1/2}\right)}, 1\right), \tag{A.1.15}$$

$$\mathbf{z_4^2} = \left(\frac{K_2}{K_3 - K_1}, 1\right). \tag{A.1.16}$$

The eigenvalues of $(h_5, 0)$ are,

$$\nu_5^1 = \frac{K_1}{K_3} - 1, \tag{A.1.17}$$

$$\nu_5^2 = \frac{2}{1 - K_2K_3A^{-1/2}}, \tag{A.1.18}$$

where the corresponding eigenvectors are,

$$\mathbf{z_5^1} = \left(\frac{-K_2\left(2K_1 + K_2\left(K_3 - 2\right) - 4K_3 - A^{1/2}\right)}{K_3\left(2K_1 + K_2\left(K_3 - 4\right) - 2K_3 - A^{1/2}\right)}, 1\right), \tag{A.1.19}$$

$$\mathbf{z_5^2} = \left(\frac{K_2}{K_3 - K_1}, 1\right). \tag{A.1.20}$$

A.2 Cytoplasmic male sterility

(h_2,0) and (h_3,0) are still equilibria for the case of cytoplasmic male sterility ($K_1 > 0$, $K_2 = 0$ and $K_3 > 0$). Though, (h_4,f_4) and (h_5,f_5) are not. For the special case $K_3 = K_1$, a curve of equilibrium points exists given by equation (5.3.12). The eigenvalues from the linear stability analysis of points on this curve are given by,

$$\nu_6^1 = 0, \tag{A.2.1}$$

$$\nu_6^2 = 2 - K_1h, \tag{A.2.2}$$

where the hermaphrodite density h refers to the hermaphrodite density on the equilibrium curve. The corresponding eigenvectors are,

$$\mathbf{z_6^1} = \left(\frac{K_1 h^2}{1 - K_1 h^2}, 1\right), \tag{A.2.3}$$

$$\mathbf{z_6^2} = \left(\frac{-K_1 h^2}{1 + K_1 h\,(h-1)}, 1\right), \tag{A.2.4}$$

again the hermaphrodite density h refers to the hermaphrodite density on the equilibrium curve.

References

[1] C. Darwin. *On the Origin of Species*. Harvard University Press, 1964.

[2] W Bateson. *Mendel's Principles of Heredity*. Cambridge University Press, 1909.

[3] J. Huxley. *Evolution : the modern synthesis*. Allen and Unwin, 3rd edition, 1974.

[4] S. A. Kauffman. *The Origins of Order: Self Organization and Selection in Evolution*. Oxford University Press, 1993.

[5] B. Drossel. Biological evolution and statistical physics. *Advances In Physics*, 50(2):209–295, March 2001.

[6] Orjan Carlborg and Chris S. Haley. Epistasis: too often neglected in complex trait studies? *Nature Reviews Genetics*, 5(8):618–625, August 2004.

[7] G. C. Williams. Pleiotropy, natural-selection, and the evolution of senescence. *Evolution*, 11(4):398–411, 1957.

[8] T. J. P. Penna. A bit-string model for biological aging. *Journal Of Statistical Physics*, 78(5-6):1629–1633, March 1995.

[9] C. F. Taylor and P. G. Higgs. A population genetics model for multiple quantitative traits exhibiting pleiotropy and epistasis. *Journal Of Theoretical Biology*, 203(4):419–437, April 2000.

[10] J. S. S. Martins, S. M. de Oliveira, and G. A. de Medeiros. Simulated ecology-driven sympatric speciation. *Physical Review E*, 6402(2):021906, August 2001.

[11] D. S. Falconer. *Intro to quantitative genetics*. Longman Scientific and Technical, 1989.

[12] D. Roff. Evolutionary quantitative genetics: Are we in danger of throwing out the bably with the bathwater? *Annales Zoologici Fennici*, 40:315–320, 2003.

[13] M. S. Kang, editor. *Quantitative genetics, genomics and plant breeding*. Cabi Publishing, 2002.

[14] H. Ellegren and B. C. Sheldon. Genetic basis of fitness differences in natural populations. *Nature*, 452(7184):169–175, March 2008.

[15] J. von Neumann and O. Morgenstern. *Theory of games and economic behavior*. Princeton University Press, 1944.

[16] J. F. Nash. Equilibrium points in n-person games. *Proceedings Of The National Academy Of Sciences Of The United States Of America*, 36(1):48–49, 1950.

[17] J. Nash. Non-cooperative games. *Annals Of Mathematics*, 54(2):286–295, 1951.

[18] J. Maynard Smith. *Evolution and the Theory of Games*. Cambridge University Press, 1982.

[19] J. Maynard Smith and G. R. Price. Logic of animal conflict. *Nature*, 246 (5427):15–18, 1973.

[20] B. Sinervo and C. M. Lively. The rock-paper-scissors game and the evolution of alternative male strategies. *Nature*, 380(6571):240–243, March 1996.

[21] T. L. Vincent and J. S. Brown. *Evolutionary Game Theory, Natural Selection, and Darwinian Dynamics*, chapter Darwinian Dynamics, pages 112–150. Cambridge University Press, 2005.

[22] I. Eshel. Evolutionary and continuous stability. *Journal of Theoretical Biology*, 103(1):99–111, 1983.

[23] J. Hofbauer and K. Sigmund. *Evolutionary Games and Population Dynamics*. Cambridge University Press., 1998.

[24] D. Stauffer. *Biological Evolution and Statistical Physics*. Springer, Berlin, 2002.

[25] M. Rose. *Evolutionary Biology of Aging*. Oxford University Press, New York, 1991.

[26] P. B. Medawar. *An Unsolved Problem of Biology*. H. K. Lewis, London, 1952.

[27] B. Charlesworth. Patterns of age-specific means and genetic variances of mortality rates predicted by the mutation-accumulation theory of ageing. *Journal Of Theoretical Biology*, 210(1):47–65, May 2001.

[28] T. J. P. Penna, S. M. Deoliveira, and D. Stauffer. Mutation accumulation and the catastrophic senescence of the pacific salmon. *Physical Review E*, 52(4):R3309–R3312, October 1995.

[29] A. Laszkiewicz, S. Szymczak, and S. Cebrat. Prediction of the human life expectancy. *Theory In Biosciences*, 122(4):313–320, 2003.

[30] S. M. de Oliveira. A small review of the penna model for biological ageing. *Physica A*, 257(1-4):465–469, March 1998.

[31] J. B. Coe, Y. Mao, and M. E. Cates. Solvable senescence model showing a mortality plateau. *Physical Review Letters*, 89(28):288103, December 2002.

[32] V. Schwammle and S. M. de Oliveira. Simulations of a mortality plateau in the sexual penna model for biological aging. *Physical Review E*, 72(3): 031911, September 2005.

[33] J. Maynard Smith. *The Evolution of Sex*. Cambridge University Press, 1978.

[34] J. S. Sï£¡ Martins and S. Moss de Oliveira. Why sex? — monte carlo simulations of survival after catastrophes. *International Journal Of Modern Physics C*, 9:421–423, 1998.

[35] J. S. Sá Martins and Racco A. Simulated emergence of cyclic sexual-asexual reproduction. *Physica A*, pages 485–494, 2001.

[36] J. B. Coe and Y. Mao. Analytical solution of a generalized penna model. *Physical Review E*, 67(6):061909, June 2003.

[37] M. Sitarz and A. Maksymowicz. Divergent evolution paths of different genetic families in the penna model. *International Journal Of Modern Physics C*, 16(12):1917–1925, December 2005.

[38] J. B. Coe, Y. Mao, and M. E. Cates. Solvable senescence model with positive mutations. *Physical Review E*, 70(2):021907, August 2004.

[39] P. F. Verhulst. Recherches mathematiques sur la loi d'accroissement de la population. *Nouveaux Memoires de l'Academie Royale des Sciences et Belles-Lettres de Bruxelles*, 18:1–45, 1845.

[40] E. Schrodinger. The theory of drop and rise tests on brownian motion particles. *Physikalische Zeitschrift*, 16:289–295, 1915.

[41] S. Redner. *A Guide to First-Passage Processes*. Cambridge University Press, 2001.

[42] D. Makowiec, J. Dabkowski, and M. Groth. The eve effect in the penna model of biological ageing. *Physica A*, 273(1-2):169–181, November 1999.

[43] D. Botstein and N. Risch. Discovering genotypes underlying human phenotypes: past successes for mendelian disease, future approaches for complex disease. *Nature Genetics*, 33:228–237, 2003.

[44] A. Rocchi, S. Pellegrini, G. Siciliano, and L. Murri. Causative and susceptibility genes for alzheimer's disease: a review. *Brain Research Bulletin*, 61 (1):1–24, June 2003.

[45] M. A. Permutt, J. Wasson, L. Love-Gregory, J. Y. Ma, G. Skolnick, B. Suarez, J. Lin, and B. Glaser. Searching for type 2 diabetes genes on chromosome 20. *Diabetes*, 51:S308–S315, 2002.

[46] J. N. Hirschhorn and M. J. Daly. Genome-wide association studies for common diseases and complex traits. *Nature Reviews Genetics*, 6(2):95–108, 2005.

[47] C. S. Carlson, M. A. Eberle, L. Kruglyak, and D. A. Nickerson. Mapping complex disease loci in whole-genome association studies. *Nature*, 429 (6990):446–452, 2004.

[48] J. Maynard Smith. Theory of games and evolution of animal conflicts. *Journal Of Theoretical Biology*, 47(1):209–221, 1974.

[49] T. L. Vincent, M. V. Van, and B. S. Goh. Ecological stability, evolutionary stability and the ess maximum principle. *Evolutionary Ecology*, 10(6):567–591, November 1996.

[50] Y. Cohen, T. L. Vincent, and J. S. Brown. A g-function approach to fitness minima, fitness maxima, evolutionarily stable strategies and adaptive landscapes. *Evolutionary Ecology Research*, 1(8):923–942, December 1999.

[51] T. L. Vincent, Y. Cohen, and J. S. Brown. Evolution via strategy dynamics. *Theoretical Population Biology*, 44(2):149–176, October 1993.

[52] P.A. Abrams, H. Matsuda, and Y. Harada. Evolutionarily unstable fitness

maxima and stable fitness minima of continuous traits. *Evolutionary Ecology*, 7(5):465–487, 1993.

[53] E. L. Charnov. Simultaneous hermaphroditism and sexual selection. *Proceedings of the National Academy of Sciences of the United States of America*, 76 (5):2480–2484, 1979.

[54] G. Arnqvist and L. Rowe. *Sexual Conflict*. Princeton University Press, 2005.

[55] N. K. Michiels. *Sperm competition and sexual selection*, chapter Mating conflicts and sperm competition in simultaneous hermaphrodites, pages 219–254. London: Academic Press, 1998.

[56] E. H. Morrow, G. Arnqvist, and S. Pitnick. Adaptation versus pleiotropy: why do males harm their mates? *Behavioral Ecology*, 14(6):802–806, November 2003.

[57] R. A. Johnstone and L. Keller. How males can gain by harming their mates: Sexual conflict, seminal toxins, and the cost of mating. *American Naturalist*, 156(4):368–377, October 2000.

[58] C. M. Lessells. Why are males bad for females? models for the evolution of damaging male mating behavior. *American Naturalist*, 165(5):S46–S63, May 2005.

[59] G. A. Parker. *Sexual selection and reproductive competition in insects*, chapter Sexual selection and sexual conflict. London : Academic Press, 1979.

[60] T. Chapman, L. F. Liddle, J. M. KalbB, M. F. Wolfner, and L. Partridge. Cost of mating in drosophila-melanogaster females is mediated by male accessory-gland products. *Nature*, 373(6511):241–244, January 1995.

[61] J. E. Lloyd. Mating-behavior and natural-selection. *Florida Entomologist*, 62 (1):17–34, 1979.

[62] N. K. Michiels and L. J. Newman. Sex and violence in hermaphrodites. *Nature*, 391(6668):647–647, February 1998.

[63] J. M. Koene and R. Chase. Changes in the reproductive system of the snail helix aspersa caused by mucus from the love dart. *Journal of Experimental Biology*, 201(15):2313–2319, August 1998.

[64] M. A. Landolfa, D. M. Green, and R. Chase. Dart shooting influences paternal reproductive success in the snail helix aspersa (pulmonata, stylommatophora). *Behavioral Ecology*, 12(6):773–777, November 2001.

[65] W.U. Blanckenhorn, D.J. Hosken, O.Y. Martin, C. Reim, Y. Teuschl, and P.I. Ward. The costs of copulating in the dung fly sepsis cynipsea. *Behavioral Ecology*, 13(3):353–358, 2002.

[66] Helen S. Crudgington and Mike T. Siva-Jothy. Genital damage, kicking and early death. *Nature*, 407(6806):855–856, October 2000.

[67] N. K. Michiels and J. M. Koene. Sexual selection favors harmful mating in hermaphrodites more than in gonochorists. *Integrative and Comparative Biology*, 46(4):473–480, August 2006.

[68] E. L. Charnov. Sperm competition and sex allocation in simultaneous hermaphrodites. *Evolutionary Ecology*, 10(5):457–462, September 1996.

[69] J. M. Greeff and N. K. Michiels. Sperm digestion and reciprocal sperm transfer can drive hermaphrodite sex allocation to equality. *American Naturalist*, 153(4):421–430, April 1999.

[70] W. R. Bryan and M. B. Shimkin. Quantitative analysis of dose-response data obtained with three carcinogenic hydrocarbons in strain c3h male mice. *Journal of the National Cancer Institute*, 3:503–531, 1943.

[71] S. D. Murphy and K. L. Cheever. Effect of fedding insecticidesinhibition of carboxyesterase and cholinesterase activities in rats. *Archives of Environmental Health*, 17(5):749, 1968.

[72] A.J. Bateman. Intra-sexual selection in drosophila. *Heredity*, 2(3):349–68, 1948.

[73] H. T. Odum and W. C. Allee. A note on the stable point of populations showing both intraspecific cooperation and disoperation. *Ecology*, 35(1): 95–97, 1954.

[74] D. S. Boukal and L. Berec. Single-species models of the allee effect: Extinction boundaries, sex ratios and mate encounters. *Journal OF Theoretical Biology*, 218(3):375–394, October 2002.

[75] M. A. Lewis and P. Kareiva. Allee dynamics and the spread of invading organisms. *Theoretical Population Biology*, 43(2):141–158, April 1993.

[76] S. M. Eppley and L. K. Jesson. Moving to mate: the evolution of separate and combined sexes in multicellular organisms. *Journal Of Evolutionary Biology*, 21(3):727–736, May 2008.

[77] R. Durrett. Stochastic spatial models. *SIAM Review*, 41(4):677–718, December 1999.

[78] R. Durrett and S. A. Levin. Stochastic spatial models a users guide to ecological applications. *Philosophical Transactions of the Royal Society of London Series B — Biological Sciences*, 343(1305):329–350, February 1994.

[79] F. Schlogl. Chemical reaction models for nonequilibrium phase-transitions. *Zeitschrift Fur Physik*, 253(2):147–&, 1972.

[80] J. A. Stewart-Cox, N. F. Britton, and M. Mogie. Pollen limitation or mate search need not induce an allee effect. *Bulletin Of Mathematical Biology*, 67 (5):1049–1079, September 2005.

[81] K. Tainaka, T. Hayashi, and J. Yoshimura. Sustainable sex ratio in lattice populations. *Europhysics Letters*, 74:554, 2006.

[82] D. Liu, X. F. Guo, and J. W. Evans. Quadratic contact process: Phase separation with interface-orientation-dependent equistability. *Physical Review Letters*, 98(5):050601, February 2007.

[83] X. F. Guo, D. J. Liu, and J. W. Evans. Generic two-phase coexistence, relaxation kinetics, and interface propagation in the quadratic contact process: Simulation studies. *Physical Review E*, 75(6):061129, June 2007.

[84] B. Dennis. Allee effects in stochastic populations. *OIKOS*, 96(3):389–401, March 2002.

[85] A. Windus and H. J. Jensen. Allee effects and extinction in a lattice model. *Theoretical Population Biology*, 72(4):459–467, December 2007.

[86] A. Richards. *Plant breeding systems*. George Allen and Unwin, London, 1986.

[87] M. F. Bailey and L. F. Delph. A field guide to models of sex-ratio evolution in gynodioecious species. *Oikos*, 116:1609–1617, 2007.

[88] A. M. Chaudhury. Nuclear genes-controlling male-fertility. *Plant Cell*, 5 (10):1277–1283, October 1993.

[89] D. Lewis. Male sterility in natural populations of hermaphrodite plants. *New Phytologist*, 40:56–63, 1941.

[90] P. S. Schnable and R. P. Wise. The molecular basis of cytoplasmic male sterility and fertility restoration. *Trends in Plant Science*, 3:175–180, 1998.

[91] D. G. Lloyd. Evolutionarily stable sex-ratios and sex allocations. *Journal of Theoretical Biology*, 105(3):525–539, 1983.

[92] E. L. Charnov. *The Theory of Sex Allocation*. Princeton University Press, 1982.

[93] J. A. Stewart-Cox, N. F. Britton, and M. Mogie. Space mediates coexistence of females and hermaphrodites. *Bulletin Of Mathematical Biology*, 67(6): 1273–1302, November 2005.

[94] D. G. Lloyd. Theoretical sex-ratios of dioecious and gynodioecious angiosperms. *Heredity*, 32(FEB):11–34, 1974.

[95] S. Maurice, D. Charlesworth, C. Desfeux, D. Couvet, and P. H. Gouyon. The evolution of gender in hermaphrodites of gynodioecious populations with nucleocytoplasmic male-sterility. *Proceedings Of The Royal Society Of London Series B — Biological Sciences*, 251(1332):253–261, March 1993.

[96] J. R. Kohn. Sex-ratio, seed production, biomass allocation, and the cost of male function in cucurbita-foetidissima (cucurbitaceae). *Evolution*, 43(7): 1424–1434, 1989.